

**MODELLING AND ANALYSIS OF A
STANDALONE PHOTO VOLTAIC / MICRO
TURBINE / ULTRA CAPACITOR HYBRID
SYSTEM**

Thesis

Submitted in partial fulfilment of the requirements for the degree of

DOCTOR OF PHILOSOPHY

by

BASAVARAJ .S. SHALAVADI



DEPARTMENT OF ELECTRICAL AND ELECTRONICS ENGINEERING

NATIONAL INSTITUTE OF TECHNOLOGY KARNATAKA

SURATHKAL, MANGALORE - 575 025

JULY, 2018

DECLARATION

by the Ph.D. Research Scholar

I hereby *declare* that the Research Thesis entitled **Modelling and Analysis of a Standalone Photo Voltaic / Micro Turbine / Ultra Capacitor Hybrid System**, which is being submitted to the **National Institute of Technology Karnataka, Surathkal** in partial fulfilment of the requirements for the award of the Degree of **Doctor of Philosophy** in department of Electrical and Electronics Engineering is a *bonafide report of the research work carried out by me*. The material contained in this Research Thesis has not been submitted to any University or Institution for the award of any degree.

BASAVARAJ .S. SHALAVADI

(110655EE11F01)

(Register Number, Name & signature of the Research Scholar)

Department of Electrical and Electronics Engineering

Place: NITK-Surathkal

Date:

CERTIFICATE

This is to certify that the Research Thesis entitled **Modelling and Analysis of a Standalone Photo Voltaic / Micro Turbine / Ultra Capacitor Hybrid System** submitted by **BASAVARAJ S. SHALAVADI** (Register Number, 110655EE11F01) as the record of the research work carried out by him, is *accepted as the Research Thesis submission* in partial fulfilment of the requirements for the award of degree of **Doctor of Philosophy**.

(Prof. Udaykumar R. Y.)

Research Guide

(Name and Signature with Date and Seal)

Chairman-DRPC

(Signature with Date and Seal)

ACKNOWLEDGEMENTS

It gives me immense pleasure and great sense of satisfaction to express my heartfelt gratitude to those who made this dissertation possible.

I take this opportunity to sincerely thank my research supervisor Prof. Udaykumar R.Y. for all his invaluable guidance, patience, encouragement, timely advice and support. He has been a constant source of inspiration throughout this journey. I feel proud to have worked under his guidance.

I thank National Institute of Technology Karnataka for giving me an opportunity for doing research. I wish to thank my research progress assessment committee (RPAC) members Dr. Ashwini Chaturvedi and Dr. K B Kiran, for their constructive feedback and guidance from research problem definition stage to thesis submission stage. Without their help thesis would not have taken this shape.

I would like to thank Prof. K.P.Vittal and Mr. Jora M. Gonda, former HOD for providing the necessary resources in the department to carry out my research. Also, I would like to thank HOD, Vinatha U for encouragement and providing valuable suggestions.

I take this opportunity to thank all teaching and non-teaching staff of EEE Department, NITK Surathkal.

I express my gratitude and thanks to the Management, Principal and HOD of SDMCET, Dharwad for deputing me to pursue Doctoral studies at NITK Surathkal.

My stay at NITK Surathkal was a sweet and memorable in the company of my fellow researchers who never let me know that I am away from home. Big thanks to all the research scholars.

Finally, I would like to thank my Guru, Family members for their patience, care and love which drew me with inspiration to carry out my research.

BASAVARAJ .S. SHALAVADI

ABSTRACT

Nowadays the distributed generation is being vastly implemented due to its various advantages. Generally a non renewable source is connected in parallel to a renewable source. Normally Photo Voltaic (PV) generation gives the power necessary by the load. The output of the PV is varying due to various reasons like temperature, irradiation, etc. Distributed generation using micro turbine is a realistic solution because of its friendliness with environment, small in size and high efficiency of energy. If the load is more than PV power capability, micro turbine supplies the remaining power. Due to the varying load conditions, the micro turbine practically compensates all the PV fluctuations of power. Even so, to reduce the fast fluctuations of power, one need to use an energy storage system like battery, ultra capacitor and flywheel etc. Ultra capacitor has been chosen, because of its high power density and very fast energy storing capability.

This thesis documents the simulation and analysis of a standalone Photovoltaic / Micro turbine / Ultra capacitor hybrid system using MATLAB/SIMULINK as its simulation software. The system is implemented based on the concept of a parallel hybrid configuration.

In the first phase of the work, each individual Photovoltaic / Micro turbine system / Ultra capacitor components were analysed using mathematical equations and modelled for software simulation. The simulation was done in discrete time domain and the resulting waveforms are shown in the report.

In the second phase of the work, each individual system components were combined to form the overall Photovoltaic / Micro turbine / Ultra capacitor hybrid system. To measure the performance, the overall system is tested for different disturbances like variation in Temperature, irradiation profile and variation in load demand which normally occurs in the hybrid power system.

TABLE OF CONTENTS

LIST OF FIGURES	iv
LIST OF TABLES	v
ABBREVIATIONS	Viii
CHAPTER 1	1
INTRODUCTION	1
1.1 DISTRIBUTED GENERATION	1
1.2 LITERATURE REVIEW	2
1.2.1 Photo Voltaic System.....	2
1.2.2 Micro Turbine Generator System.....	4
1.2.3 Ultra Capacitor System	5
1.2.4 Hybrid System.....	6
1.3 RESEARCH OBJECTIVES	7
1.4 THESIS ORGANISATION	7
CHAPTER 2	9
PHOTO VOLTAIC SYSTEM	9
2.1 SOLAR CELL CONSTRUCTION	9
2.2 Materials Used in PV Cell	10
2.3 PV Modeling	11
2.4 Estimation of Parameters:	14
2.5 MPPT Algorithm	15
2.5.1 Incremental Conductance Algorithm.....	16
2.6 Boost Converter	17
2.7 SIMULATION RESULTS	19
2.71 Photovoltaic System	19
2.72 Parameter Estimation	19

2.73 Simulink Model of PV Array.....	22
2.74 PV Model with MPPT	26
CHAPTER 3.....	29
MICRO TURBINE	29
3.1 Types of Micro Turbine Systems	29
3.2 Modeling of MTG.....	31
3.2.1 Speed and Acceleration Control	31
3.2.2 Fuel Control.....	32
3.2.3 Compressor and Turbine.....	32
3.2.4 Temperature Control.....	33
3.3 Permanent Magnet Synchronous Generator	33
3.4 Power Conditioning System	35
3.4.1 Three Phase Diode Bridge Rectifier	35
3.4.2 Three Phase PWM Inverter	36
3.4.2.1 VF Control	37
3.4.2.2 Sinusoidal Pulse Width Modulation	38
3.5 Filter	39
3.6 Simulation results.....	40
3.7 ULTRA CAPACITOR SYSTEM.....	45
3.71 UC Modeling.....	45
3.72 Bidirectional DC-DC Converter	46
CHAPTER 4.....	49
HYBRID SYSTEM	49
4.1 PV/MTG/UCHybrid System	51
4.2 PV/MTG Hybrid System	60
CHAPTER 5.....	61
CONCLUSION AND FUTURE SCOPE	61
5.1 Recap of work done.....	61
5.2 Scope for future work	62

APPENDIX.....	63
REFERENCES.....	65
REFERENCES.....	65
LIST OF PUBLICATIONS	69
CURRICULUM VITAE.....	70

LIST OF FIGURES

Figure 2.1: Solar cell construction	10
Figure 2.2: Ideal single diode model.....	11
Figure 2.3: Simplified single diode model.....	11
Figure 2.4: Single diode model	12
Figure 2.5: The equivalent circuit of PV array	12
Figure 2.6: I-V characteristic of the array.....	13
Figure 2.7: P-V characteristic of the array.....	13
Figure 2.8: Parameter estimation algorithm.....	15
Figure 2.9: Incremental conductance algorithm.....	16
Figure 2.10: Boost Converter.....	17
Figure 2.11: Boost converter waveforms	18
Figure 2.12: I-V curve - adjusting R_s and R_p	20
Figure 2.13: P-V curve - adjusting peak power	21
Figure 2.14: Adjusted I-V curve	21
Figure 2.15: Adjusted P-V curve	22
Figure 2.16: Simulink PV array model	22
Figure 2.17: PV model subsystem	23
Figure 2.18: Calculation of I_m	23
Figure 2.19: Calculation of I_{pv}	23
Figure 2.20: Calculation of I_o	24
Figure 2.21: I-V model curves for different temperatures	24
Figure 2.22: P-V model curves for different temperatures	24
Figure 2.23: I-V model curves for different irradiances	25
Figure 2.24: P-V model curves for different irradiances	25
Figure 2.25: Simulink PV system model	26
Figure 2.26: MPPT subsystem	26
Figure 2.27: Simulink model of IncCond	27
Figure 2.28: Boost converter implemented in simulink.....	27
Figure 2.29: Temperature and irradiation variations.....	28

Figure 2.30: Waveforms of the MPP voltage, current and power.....	28
Figure 3.1: Single shaft Micro Turbine	30
Figure 3.2: Split shaft Micro Turbine	30
Figure 3.3: Block diagram of a micro turbine.....	31
Figure 3.4: Speed Control	31
Figure 3.5: Fuel Control system.....	32
Figure 3.6: Compressor and Turbine system	33
Figure 3.7: Temperature Control system	33
Figure 3.8: d axis equivalent circuit.....	34
Figure 3.9: q axis equivalent circuit.....	34
Figure 3.10: 3 Phase diode bridge rectifier	35
Figure 3.11: 3 Phase diode bridge rectifier waveforms	36
Figure 3.12: Three phase inverter	37
Figure 3.13: VF control system.....	37
Figure 3.14: Sinusoidal pulse width modulation.....	38
Figure 3.15: LC low pass filter	39
Figure 3.16: Frequency response of LC low pass filter	39
Figure 3.17: Micro turbine system	40
Figure 3.18: Micro turbine generator subsystem	41
Figure 3.19: Micro turbine subsystem	41
Figure 3.20: Voltage control subsystem.....	42
Figure 3.21: Speed, Torque and Power of Micro turbine	42
Figure 3.22: DC link voltage,current and power.....	42
Figure 3.23: Inverter Vab line voltage	43
Figure 3.24: Load phase current and voltage waveforms	43
Figure 3.25: Part of load phase voltage and current waveforms	44
Figure 3.26: Load power	44
Figure 3.27: Ultra capacitor equivalent circuit	46
Figure 3.28: Bidirectional DC-DC converter.....	47
Figure 3.29: Bidirectional dc-dc converter control system.....	47
Figure 4.1: PV/MTG/UC hybrid standalone system.....	50

Figure 4.2: PV/MTG/UC hybrid system	51
Figure 4.3: The Micro turbine subsystem	51
Figure 4.4: Buck converter simulink model.....	52
Figure 4.5: Buck converter PI control simulink model.....	52
Figure 4.6: Ultra capacitor subsystem.....	52
Figure 4.7: Ultra capacitor bank model.....	53
Figure 4.8: Bidirectional DC-DC converter.....	53
Figure 4.9: Bidirectional DC-DC converter control model	53
Figure 4.10: VF control.....	54
Figure 4.11: MPPT voltage,current and power waveforms	54
Figure 4.12: PV output voltage, current and power waveforms	54
Figure 4.13: Speed, Tourque and Power of MTG.....	55
Figure 4.14: MTG output voltages, current and power.....	55
Figure 4.15: Ultra capacitor voltages, current and power	56
Figure 4.16: Inverter Vab line voltage	56
Figure 4.17: Load Vabc and Iabc waveforms	57
Figure 4.18: Part of Vabc and Iabc	57
Figure 4.19: Load power PQ.....	58
Figure 4.20: PV/MTG hybrid system simulink model.....	59
Figure 4.21: Comparison of DC link voltages	59

LIST OF TABLES

Table 2.1: KC-200GT PV module specifications	19
Table 2.2: Adjusted parameters of PV module	19
Table 2.3: Boost converter specifications	27

ABBREVIATIONS

I_{pv}	Current generated by the incident light
I_0	Reverse saturation or leakage current of the diode
q	Electron charge ($1.60217646 \times 10^{-19}$ C)
K	Boltzmann constant ($1.3806503 \times 10^{-23}$ J/K)
T	Temperature of the $p-n$ junction
a	Diode ideality constant and
V_t	Thermal voltage of the module
R_s	Equivalent series resistance of PV module
R_p	Equivalent parallel resistance of PV module
G	Irradiation on the device surface
G_n	Nominal irradiation
$V_{oc,n}$	Nominal open-circuit voltage
$I_{sc,n}$	Nominal short-circuit current
V_{mp}	Voltage at the MPP
I_{mp}	Current at the MPP
K_V	Open-circuit voltage temperature coefficient
K_I	Short circuit current temperature coefficient
$P_{max,e}$	Maximum experimental peak output power
dV	Voltage incremental change
dI	Voltage incremental change
D	Duty cycle
ΔI_l	Load current ripple %
ΔV_o	Output voltage ripple %
LVG	Least value gate
K	Controller gain
T_1	Governor lead time constant
T_2	Governor lag time constant
Z	Governor mode constant

K_v	Valve positioner gain
K_f	Fuel system actuator gain
T_v	Valve positioner time constant
T_f	Fuel system actuator time constant
W_f	Fuel demand signal in p.u.
V_{ce}	Least amount of fuel needed
T_{CR}	Combustion reaction transport delay
T_{CD}	Compressor discharge time lag
T_R	Reference temperature
T_t	Temperature controller integration rate
T_3	Radiation shield time constant
T_4	Thermocouple time constant
$K_{4, 5}$	Radiation shield constants
T_5	Temperature controller time constant
L_q	q axis inductance
L_d	d axis inductance
R	Resistance of the stator windings
I_q	q axis current
I_d	d axis current
V_q	q axis voltage
V_d	d axis voltage
w_r	Angular velocity of the rotor
λ	Flux induced in the stator windings
p	Number of pole pairs
T_e	Electromagnetic torque
J	Combined inertia of rotor and load
F	Combined viscous friction of rotor and load
θ	Rotor angular position
T_m	Shaft mechanical torque
DG	Distributed generations
PV	Photo voltaic

STC	Standard test condition
ISDM	Ideal single diode model
SDM	Single diode model
SSDM	Simplified single diode model
EA	Evolutionary algorithms
GA	Genetic Algorithm
PSO	Particle Swarm Optimization
DE	Differential Evolution
MPPT	Maximum power point tracking
PAO	Perturb and Observe
IC	Incremental conductance
MTG	Micro turbine generator
PMSG	Permanent magnet synchronous generator
UC	Ultra capacitor
SPWM	Sinusoidal pulse width modulation
ESR	Equivalent series resistance of UC
EPR	Equivalent parallel resistance of UC
FSC	Fractional short circuit current
FOC	Fractional open circuit voltage
RCC	Ripple correction control

CHAPTER 1

INTRODUCTION

1.1 DISTRIBUTED GENERATION

The key drivers for turning attention towards the use of renewables for electricity generation includes continuously increasing demand for energy, depleting fossil fuels and threat of increased pollution adversely affecting the environment. The potential extraction of the energy from the renewable resources help achieving the considerable reductions in the pollution levels and addressing the climate changing related issues. In contrary, the energy from renewable sources viz. solar energy, wind energy etc. is flexible when operated independently and capacity is bottle neck till the development of appropriate technologies for scaling up. However, with the current generation technologies, there is a scope to achieve sustainable energy from these flexible energy sources through proper integration.

The remote and rural areas suffer from energy comforts due to difficulty of installing infrastructure though intended to provide power with required capital investment from the central grid. In some cases it may not be economically viable due to the high investment on transmission lines and higher transmission losses while providing power from the central grid. The liberalization policy having led to deregulation of electricity market helped exploring the possibility of setting up hybrid systems as standalone units acting as distributed generations (DG) sources.

This has led to the concept of integrating hybrid generation units involving conventional or non-conventional sources of energy or both, where two or more standalone generation systems operating in parallel such that they are supplementing each other or one another. A typical hybrid generation system, call for the use of

power electronic devices for functioning and interfacing among different generating units and with the distribution network (in grid connected operation mode).

The literature survey reveals documentation and demonstration of positive impacts on the operation of power systems involving DGs. DG is promising technology with reasonable efficiency, environmentally acceptable and fairly reliable power source. Suitably modelling these DGs, resulting in hybrid generation systems, need to be studied for their operation and impact on power systems.

1.2 LITERATURE REVIEW

This thesis deals with the development of a simulation model to determine the performance of a stand-alone hybrid generation system involving Photo voltaic energy conversion system, a micro turbine generation system and an ultra capacitor system. This section presents a brief review of related published work on the Photo voltaic/Micro turbine/Ultra capacitor hybrid systems. The work referred in the following sections is used for modelling of individual components of the hybrid system.

1.2.1 Photo Voltaic System

The PV models can be categorized into five main types. Of the many, the simplest model is the ideal single diode model (ISDM) (Yousef Mahmoud et al. 2012). Though simple, it does not give accurate characteristics at MPP. Because of accuracy single-diode model (SDM) is preferred for conducting PV studies (Marcelo Gradella Villalva et al. 2009). Some studies neglect shunt resistance to have less complexity. Although the complexity is reduced, it exhibits deviations when subjected to temperature variations (Z. Salam 2010). Few models use 2 or 3 diodes with increased complexity, however, exhibit more accuracy (Kashif Ishaque et al.2011, Kensuke Nishiokaa et al. 2007). Few models are available considering the solar cell structure

(amorphous or mono crystalline or poly crystalline, Ulrich Stutenbaeumer et al. 1999). The model selection depends on the required accuracy. In this work Single diode model is used as it gives accurate estimates with ease of implementation.

Single Diode Model (SDM) requires minimum five parameters to develop the PV model for simulation. The model includes five nonlinear equations, the solution of these equations help determining parameters. These equations are solved analytically by calculating Co-content function (Adelmo Ortiz Conde et al. 2006) or iteratively by using evolutionary algorithms (EA) methods, like Genetic Algorithm (GA), Particle Swarm Optimization (PSO) and Differential Evolution (DE) (Kashif Ishaque et al. 2011, M. Zagrouba et al. 2010, Nicolai Moldovan et al. 2009). Tuning some of the parameters such that the characteristic matches with the three operating points given by the datasheet (Marcelo Gradella Villalva et al. 2009, M. Haouari Merbaha et al. 2005). The explained method (Marcelo Gradella Villalva et al. 2009) is implemented in this work and validated.

The implementation of the PV array is shown in (Marcelo Gradella Villalva et al. 2009, Roberto F. Coelho et al. 2009) is validated in this work. The PV array output varies with the temperature and irradiation. Hence, it is required to extract the maximum power from the PV array at varying conditions like changes in temperature and irradiation. So various Maximum power point tracking (MPPT) algorithms like Perturb and Observe (PAO), Hill climbing, Incremental conductance (IC), Fractional short circuit current (FSC), Fractional open circuit voltage (FOC), Neural networks, Fuzzy logic, Ripple correction control (RCC), Current sweep and DC link capacitor droop control are available (Trishan Eram et al. 2007). The PAO is easy to implement but it gives error under varying conditions. The IC is also very easy to implement and it tracks the MPP even at varying conditions (Nevzat Onat 2010). The efficiency of PAO and IC are almost same, so IC is implemented in this thesis (D. P. Hohm et al. 2003).

The MPPT algorithm decides the duty cycle at which the DC-DC converter is to operate. Based on the duty cycle the PWM pulses are generated and applied to the

gate of the DC- DC converter (Azadeh Safari et al. 2011). There are many isolated DC- DC converters like Buck converter, Boost converter, Buck Boost converter, Cuk converter and Sepic converter (Muhammad H. Rashid 2001). Boost converter has been used in this thesis as the PV voltage needs to be increased to the DC grid voltage level for connecting PV array to DC grid.

1.2.2 Micro Turbine Generator System

Since the PV power is flexible, it is necessary to involve another DG system to match the load requirement. Distributed generation using micro turbine generator (MTG) is a realistic solution because of its friendliness with environment, compact in size, fuel flexibility, durability and high efficiency of energy (A. Al-Hinai et al. 2002).

MTG works on Brayton cycle. Single shaft MTG system can be implemented using many models like Rowen's original model, Rowen's modified model, Rowen's simplified model, IEEE model, CIGRE model, GAST governor model, Frequency dependent model. Though the derivation of the IEEE model seems to be easy, the equations are relatively complex and could cause a problem in computation time especially for large systems. A compromise arrived at between the two models. In the case of weak systems with large frequency variations the frequency dependent model should be used in particular, (Soon Kiat Yee et al. 2008).

Single shaft MTG is modelled in this work using Rowen's original model. The parameters as mentioned in (D. N. Gaonkar et al. 2006, S. R. Guda et al. 2005, Gang Li et al. 2010) is implemented.

The generator to be used is Permanent magnet synchronous generator (PMSG). Super high speed PMSM is an important component of single shaft MTG system. One of the major advantages of PMSM is the possibility of super high speed operation leading to a very small unit as the size of the machine decreases almost in directly proportion to the increase in speed. The modelling of the PMSG narrated in (D. N. Gaonkar et al. 2006, Godswill Ofualagba 2012) is implemented.

A cycloconverter or matrix converter can also be used to interface the MTG system to the grid (Hassan Nikkhajoei et al. 2005). There are different schemes for the control of the inverter, like PQ control, PV control and VF control. For a standalone system VF control is used (R N Patel et al. 2006). For a two shaft design, there is no need for such interfacing. In this thesis AC-DC-AC conversion is done by a three phase diode bridge rectifier and three phase PWM inverter combination with DC link. The starting and cooling of MTG is not considered.

1.2.3 Ultra Capacitor System

Ultra capacitors (UC) also called super capacitors. Electric double layer capacitors (EDLC) are capacitors with capacitance values greater than any other capacitor type available today. Capacitance values reaching up to 400 Farads in a single standard case size are available. The features of the ultra capacitor includes high power density, low cost per cycle, long life time, very high rates of charge and discharge, environmental friendly, good reversibility, extremely low internal resistance (ESR) and light weight (M Jayalakshmi et al. 2008).

The equivalent model of the ultra capacitor is a resistance in series with a parallel RC circuit (Santhoshakumar A et al. 2011). The design of the ultra capacitor bank required is done according to method implemented in (Prashant Kumar Soori et al. 2011, Wu Ying et al.2011). The control of the ultra capacitor is implemented by using two PI controllers for the dc voltage and the ultra capacitor current (Xiao Li et al. 2008, Jae Hoon Cho et al. 2010, Zhixue Zheng et al. 2011).

The changing load conditions will be reflecting as change in DC bus voltage. To mitigate these variations UC system will be connected to DC bus through a bidirectional converter. Bidirectional converter will facilitate power absorption as well as power feed. The design of the bidirectional DC-DC converter is done as shown in (M. Cacciato et al. 2004).

1.2.4 Hybrid System

The hybrid standalone power generating system (HSPGS) based on a wind turbine (WT) and a solar-photovoltaic (PV) array. A squirrel cage induction generator (SCIG) is coupled with a WT for electromechanical energy conversion. The frequency and amplitude of voltage at AC bus, as well as, power quality improvement at the point common coupling (PCC) are achieved by controlling the three-leg voltage source converter (VSC) using decoupled nonlinear control algorithm. A battery energy storage system (BESS) is reinforced in the hybrid system to ensure power levelling under wind, solar and load fluctuations. For obtaining the maximum power from a solar PV array and to regulate the output DC voltage, a DC-DC boost converter is controlled using perturbation and observation technique. Moreover, a dump load is tied at DC bus to ensure stability of control and to protect the BESS and solid state switches from overvoltage at DC bus during the period of fully charged battery (Bhim Singh et al. 2016).

The model predictive control (MPC) approach for voltage stability of an isolated hybrid, wind–diesel generation system based on reactive power control. This scheme consists of a synchronous generator (SG) for a diesel-generator (DG) system and an induction generator (IG) for a wind energy conversion system. A static voltage automatic regulator (VAR) compensator (SVC) is connected at terminal bus to stabilise load voltage through compensating of reactive power. Two control paths are used to stabilise load bus voltage based on MPC. The first one by controlling the total reactive power of the system that by controlling the SVC firing angle and hence the load voltage. The second control path by controlling the SG excitation voltage and hence the load bus terminal voltage. The MPC is used to determine the optimal control actions including system constraints (Ahmed M. Kassem et al. 2014).

A pulsewidth modulation (PWM) and pulse frequency modulation (PFM) hybrid modulated three-port converter (TPC) interfacing a photovoltaic (PV) source, a storage battery, and a load is proposed for a standalone PV/battery power system. The TPC is derived by integrating a two-phase interleaved boost circuit and a full-bridge LLC resonant circuit. Hence, it features a reduced number of switches, lower cost, and single-stage power conversion between any two of the three ports. With the PWM and PFM hybrid modulation strategy, the dc voltage gain from the PV to the load is wide,

the input current ripple is small, and flexible power management among three ports can be easily achieved (Xiaofeng Sun et al. 2015).

1.3 RESEARCH OBJECTIVES

In this work a MATLAB/SIMULINK model to evaluate the performance of a stand-alone hybrid generation system comprising of a photo voltaic energy conversion system, a micro turbine generation system and a ultra capacitor system is developed.

The main objectives of this work are:

- Implement a PV model in Mat lab/ Simulink:
 - Single diode model,
 - Parameter estimation (Rs and Rp),
 - MPPT algorithm (IC).
- Implement a MTG model in Mat lab/ Simulink:
 - Single shaft MTG system
- Implement a ultra capacitor model
- Develop a standalone hybrid system (PV/ MICRO TURBINE) in Matlab/ Simulink
- Develop the standalone hybrid system (PV/ MICRO TURBINE/ ULTRA CAPACITOR) in Mat lab/ Simulink

1.4 THESIS ORGANISATION

This thesis is organised as follows:

Chapter 1. Deals with the background about the proposed system and its components. The existing literature survey on these topics is reported. The research objectives and the organization of the thesis is presented at the end of the chapter.

- Chapter 2. This chapter is dedicated to the modelling and simulation of PV system. The PV cell construction, working and MPPT implementation in MATLAB/SIMULINK is included.
- Chapter 3. Gives the types of MTG and UC along with the working, Mathematical modelling and simulation of MTG and UC system in MATLAB/SIMULINK is done and their performances are analysed.
- Chapter 4. Deals with the simulation of Hybrid PV/MTG and PV/MTG/UC systems developed in MATLAB/SIMULINK and analysed the results for their performance.
- Chapter 5. Covers the summary of the work carried out briefly outlining the main contributions based on the modelling and analysis. It also enlists the scope for future investigations in the area of hybrid systems.

CHAPTER 2

PHOTO VOLTAIC SYSTEM

A solar cell is a device which directly converts sunlight into electricity. Light incident on the solar cell produces both a current and a voltage and supplies electric power. This process requires firstly, a material in which the absorption of light raises an electron to a higher energy level and secondly, the movement of this higher energy electron from the solar cell into an external circuit. In practice, nearly all photovoltaic (PV) energy conversion uses semiconductor materials in the form of a $p-n$ junction (Christiana Honsberg et al. 2000).

2.1 SOLAR CELL CONSTRUCTION

The basic construction of a solar cell is shown in the figure 2.1. The parts of the cell are as listed below:

- Anti reflective coating
- Emitter
- Base
- Front contacts and
- Rear contacts

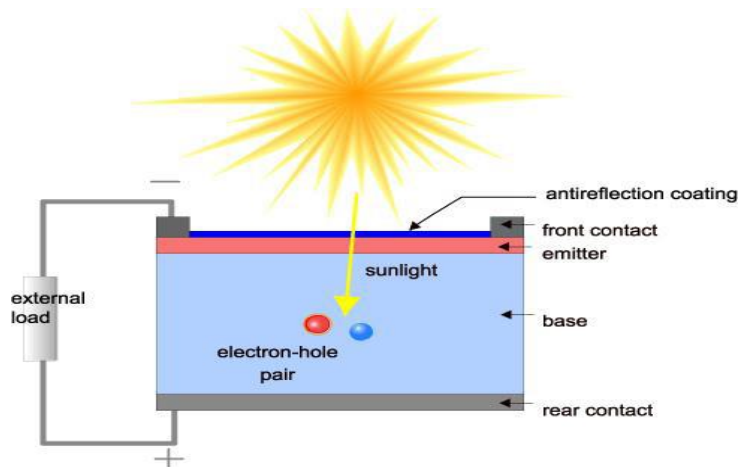


Figure 2.1: Construction details of Solar cell

2.2 Materials Used in PV Cell

The materials used in the construction of solar PV cell are as follows:

- Mono-crystal silicon
- Polycrystalline silicon
- Gallium Arsenide (GaAs)
- Cadmium Telluride (CdTe)
- Copper Indium Diselenide (CuInSe₂)

The PV industry typically makes use of mono-crystal silicon. The main technique for producing single-crystal silicon is the Czochralski (CZ) method. The presence of small grains in single-crystal silicon makes them to be more energy efficient compared to polycrystalline PV cells.

Copper Indium Diselenide (CuInSe₂) is a polycrystalline compound semiconductor made of copper, indium and selenium.

2.3 PV Modeling

PV models can be classified into five main types. They are:

- Ideal single diode model (without R_s , R_p),
- Single diode model (with R_s , R_p),
- Simplified single diode model (without R_p),
- Two diode model,
- Three diode model.

The simplest model is the ideal single-diode model (ISDM). Despite its simplicity, it does not guarantee specified performance at the MPP. The Ideal single diode model and Simplified single diode model of PV cell are as shown in figure 2.2 and 2.3 respectively.

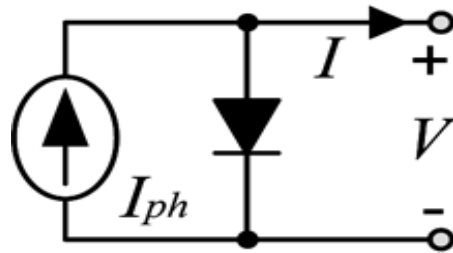


Figure 2.2: Ideal single diode model

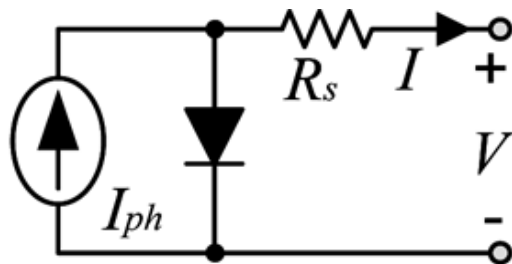


Figure 2.3: Simplified single diode model

The equivalent circuit of the one diode model of PV cell is as shown in figure 2.4.

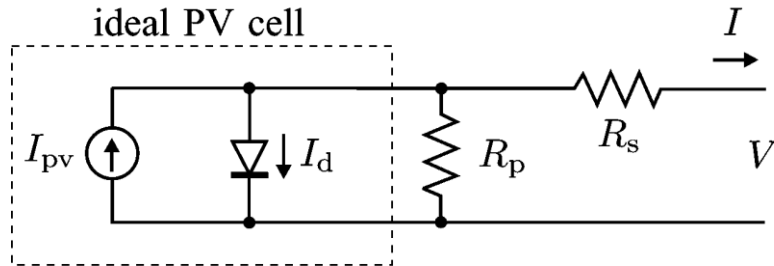


Figure 2.4: Single diode model.

The mathematical equation that describes the I-V characteristic of the photovoltaic module is as shown in equation 2.1.

$$I = I_{PV} - I_O \left[\exp \left(\frac{V+IR_S}{aV_t} \right) \right] - \frac{V+IR_S}{R_P} \quad (2.1)$$

The equivalent circuit of a PV array with N_{ser} number of modules in series and N_{par} number of modules in parallel, is as shown in fig 2.5 (Marcelo Gradella Villalva et al.2009).

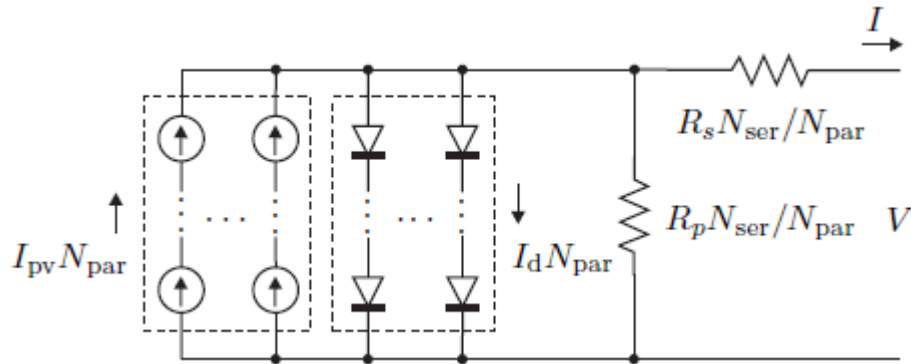


Figure 2.5: The equivalent circuit of PV array

The I-V characteristic equation of the photovoltaic array is as shown in equation 2.2.

$$I = N_{par} I_{PV} - N_{par} I_O \left[\exp \left(\frac{V+IR_S \frac{N_{ser}}{N_{par}}}{aV_t N_{ser}} \right) \right] - \frac{V+IR_S \frac{N_{ser}}{N_{par}}}{R_P \frac{N_{ser}}{N_{par}}} \quad (2.2)$$

$$I_O = \frac{I_{sc,n} + K_I \Delta T}{\exp \left(\frac{V_{oc,n} + K_V \Delta T}{aV_t} \right) - 1} \quad (2.3)$$

$$I_{PV} = (I_{PV,n} + K_I \Delta T) \frac{G}{G_n} \quad (2.4)$$

The I-V characteristic of the PV array is as shown in figure 2.6.

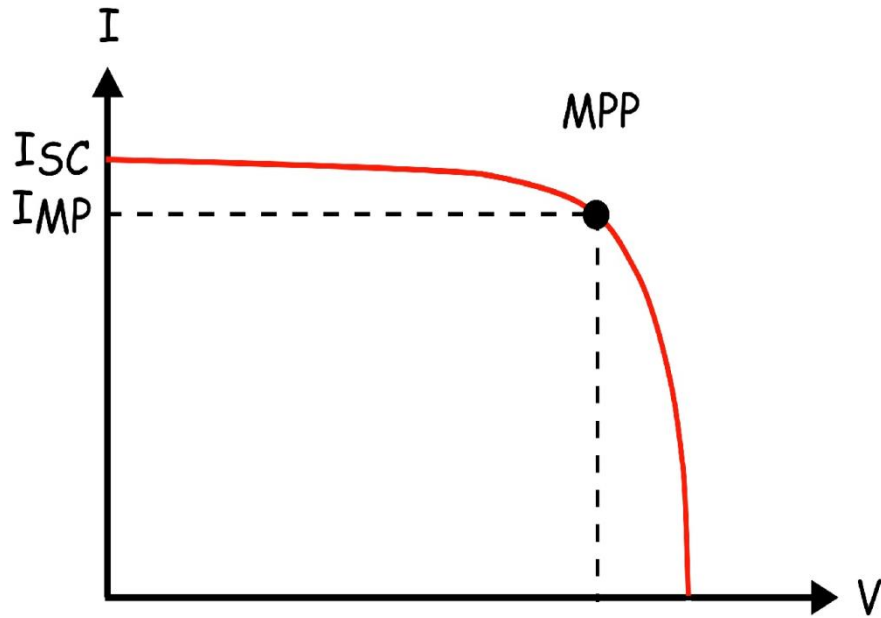


Figure 2.6: I-V characteristic of the array

The P-V characteristic of the array is as shown in figure 2.7.

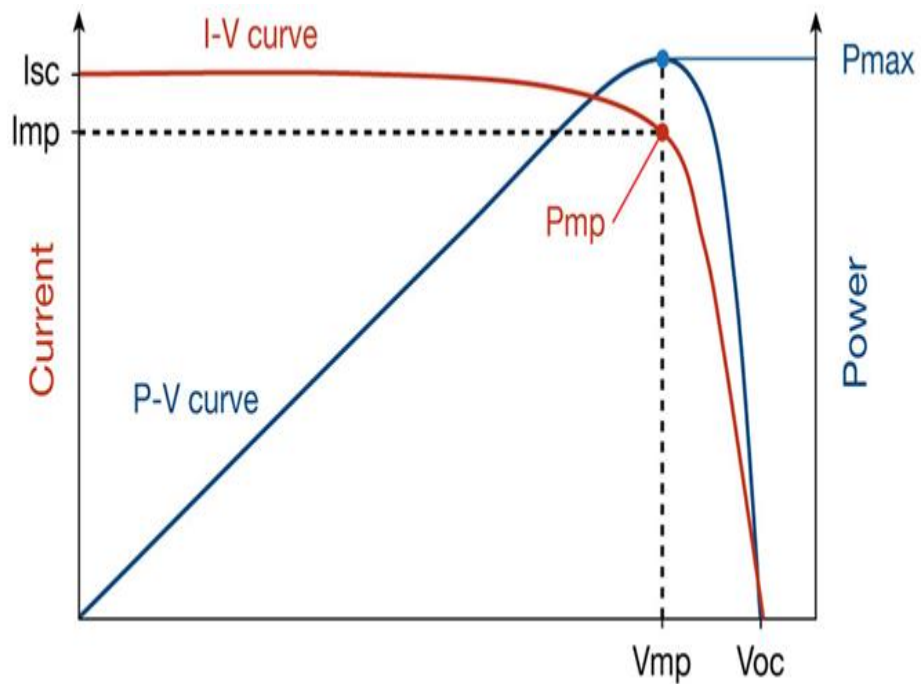


Figure 2.7: P-V characteristic of the array

2.4 Estimation of Parameters:

Manufacturers of PV arrays, instead of the $I-V$ equation, provide only a few experimental data about electrical and thermal characteristics. But, some of the parameters of PV array models require adjustment, which are not found in the manufacturer's datasheets.

The parallel resistance is calculated by equating $P_{\max,e} = P_{\max,m}$ as shown in equation 2.5.

$$R_p = \frac{V_{mp}(V_{mp} + I_{mp}R_s)}{\left\{ I_{pv}V_{mp} - I_0V_{mp} \exp \left[\frac{V_{mp} + I_{mp}R_s}{aN_s} \frac{q}{KT} \right] + I_0V_{mp} - P_{\max,e} \right\}} \quad (2.5)$$

For initial calculations, $R_s = 0$ and

$$R_{p,min} = \frac{V_{mp}}{I_{sc,n} - I_{mp}} - \frac{V_{oc,n} - V_{mp}}{I_{mp}} \quad (2.6)$$

And the nominal photo voltaic current is as shown as shown in equation 2.7.

$$I_{pv,n} = \frac{R_p + R_s}{R_p} I_{sc,n} \quad (2.7)$$

The I-V points are easily obtained by numerically solving $G(V, I) = I - F(V, I) = 0$.

To solve the above equation Newton method is used. The basic step of the algorithm is as shown in equation 2.8.

$$I = I - \frac{G(V,I)}{G(V,I)'} \quad (2.8)$$

Where $G(V,I)'$ = is the derivative of the $G(V,I)$.

The complete algorithm for parameter estimation is as shown in figure 2.8. (Marcelo Gradella Villalva et al. 2009).

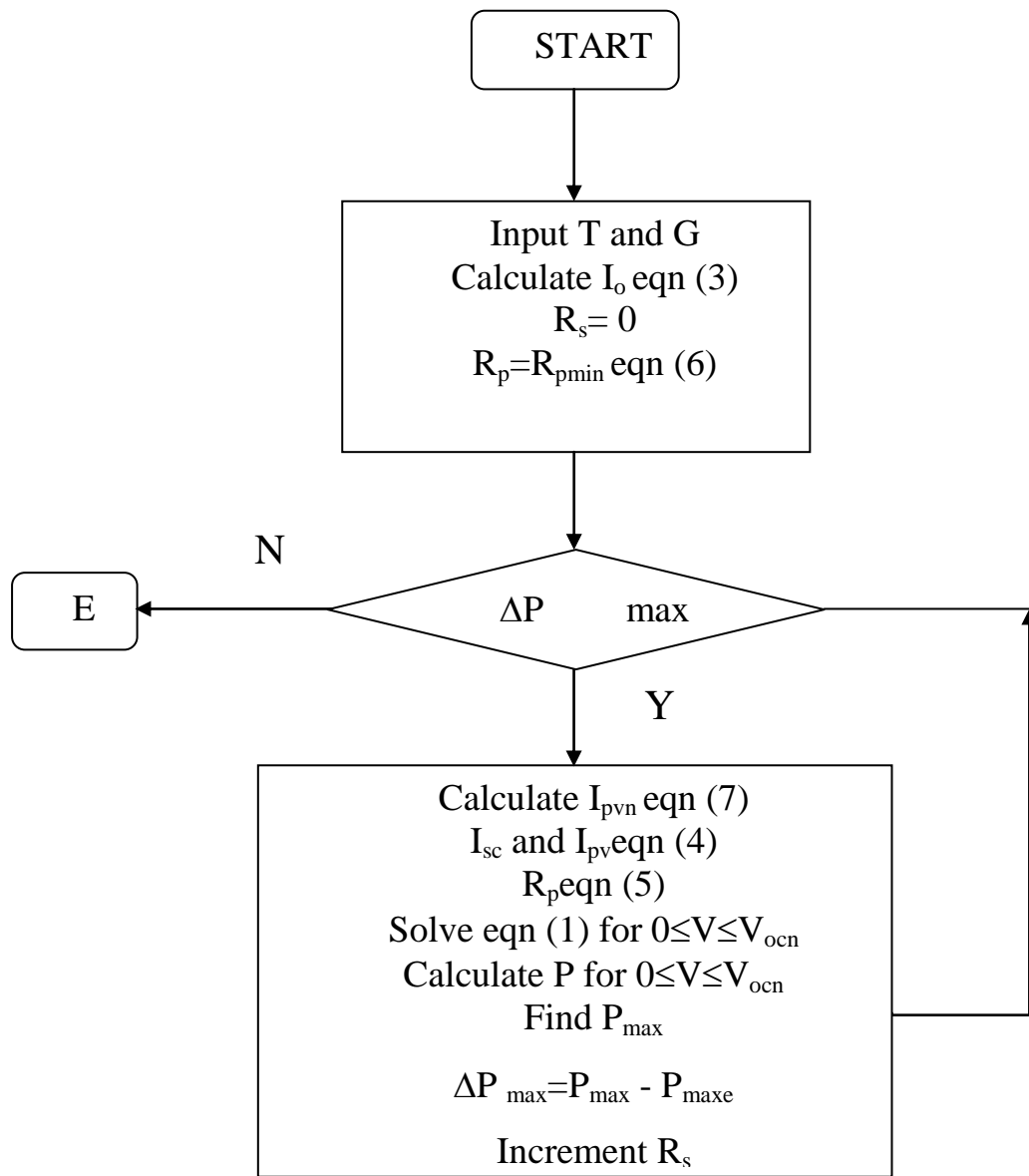


Figure 2.8: Parameter estimation algorithm

2.5 MPPT Algorithm

The efficiency of energy conversion depends mainly on the efficiency of the PV panels that generate the power. Weather conditions also influence the efficiency, which depends nonlinearly on the irradiation level and temperature.

2.5.1 Incremental Conductance Algorithm

The basic idea of Incremental Conductance (IC) is that the slope of P - V curve becomes zero at the MPP and a relative location of the operating point to the MPP can be found by looking at the slopes of P - V characteristics.

Figure 2.9 shows the Incremental Conductance algorithm.

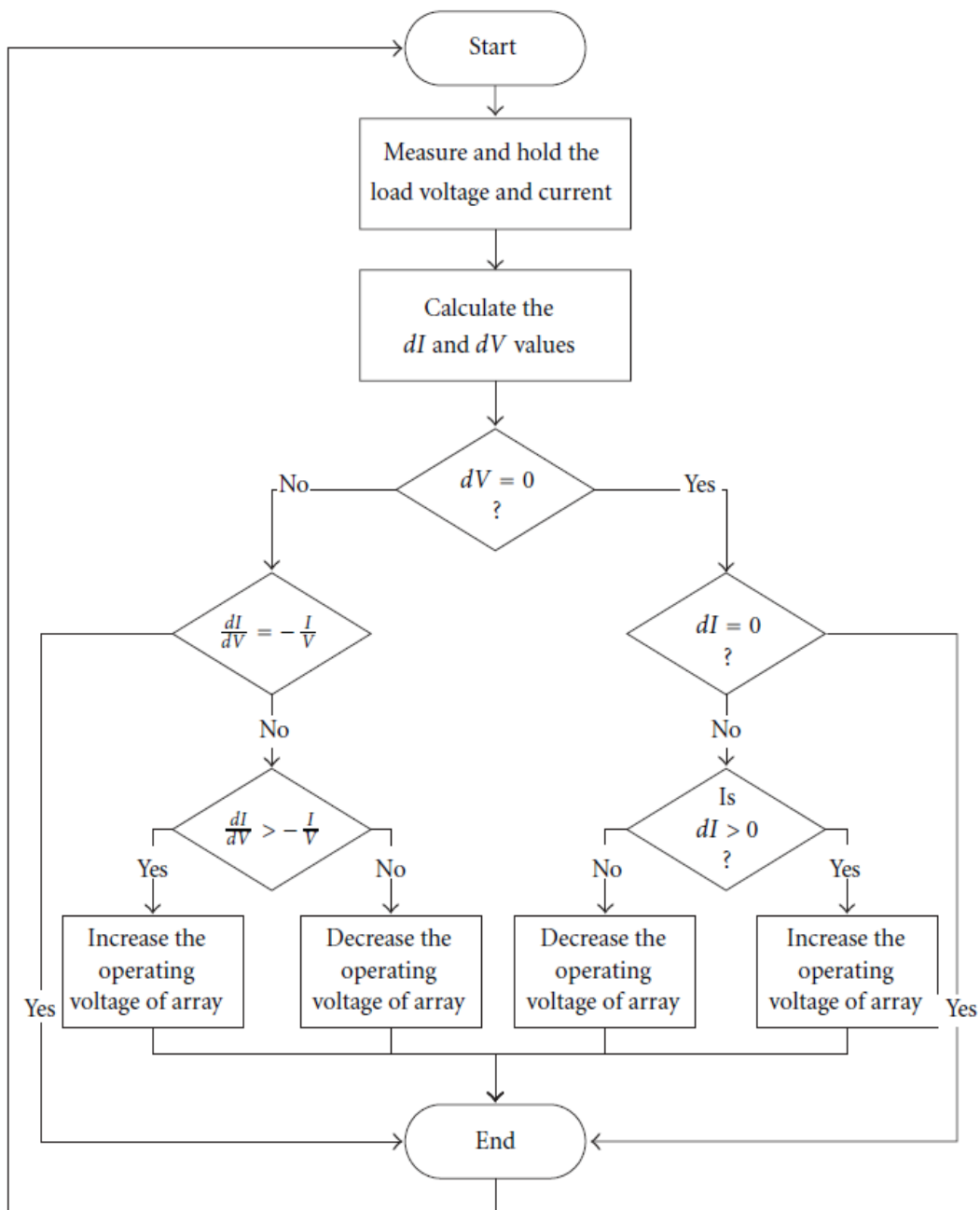


Figure 2.9: Incremental Conductance algorithm

In practice, the condition $dP/dV = 0$ (or $dI/dV = -I/V$) seldom occurs. Thus, a small margin of error (e) should be allowed, $dP/dV = \pm e$ and is obtained as shown in the equation (2.13). The value of e is optimized based on the steady-state tracking error and a risk of oscillation of the operating point.

A simple proportional integral (PI) control can then be used to drive e to zero (NevzatOnat2010).

$$\frac{i}{v} + \frac{di}{dv} = e \quad (2.9)$$

2.6 Boost Converter

The boost converter increases the input voltage to the required higher level. The boost converter configuration is as shown in the figure 2.10.

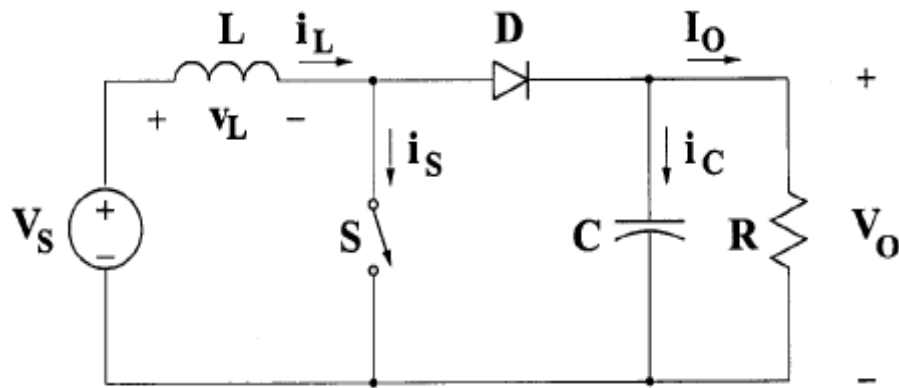


Figure 2.10: Boost Converter

The dc voltage transfer function turns out to be as shown in equation 2.10 :

$$\frac{V_o}{V_s} = \frac{1}{1 - D} \quad (2.14)$$

The average of the inductor current is same as the average source current.

$$\frac{I_s}{I_o} = \frac{1}{1 - D} \quad (2.15)$$

The converter waveforms in the CCM are as shown in figure 2.11.

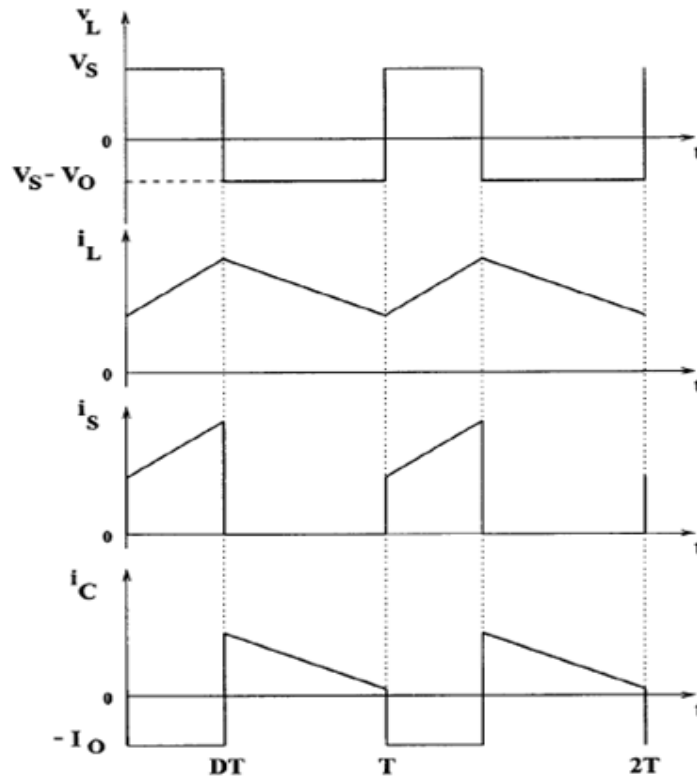


Fig 2.11: Boost converter waveforms

In each sub-period [dT and $(1-d)T$] the rate of change of current is constant. Therefore the current ripple is as shown in equation 2.12.

$$\frac{\Delta I_L}{I_L} = \frac{RD(1-D)^2}{LF} \quad (2.16)$$

. The voltage ripple is as shown in equation 2.13.

$$\frac{\Delta V_o}{V_o} = \frac{D}{RCF_s} \quad (2.17)$$

2.7 SIMULATION RESULTS

2.71 Photovoltaic System

The PV module considered here is the KYOCERA KC200GT. The specifications at nominal conditions 25°C and 1000 W/m² are shown in Table 2.1:

Table 2.1: KC200GT PV module specifications

Imp	7.61 A
Vmp	26.3 V
Pmax,e	200.143 W
Isc	8.21 A
Voc	32.9 V
Kv	-0.1230V/K
Ki	0.0032A/K
Ns	54

2.72 Parameter Estimation

The adjusted values of the KC200GT module with parameter estimation algorithm implementation are given in Table 2.2:

Table 2.2: Adjusted parameters of the PV module

Rpmin	42.966 ohm
Rp	415.405 ohm

R _{smax}	0.867 ohm
R _s	0.221 ohm
A	1.300
P _{max,m}	200.143 W
P _{max,e}	200.143 W
P _{error}	0.000
I _{pv}	8.214 A
I _{sc}	8.210A
I _{on}	0.000A

The figures 2.12 and 2.13 shows the Parameter estimation algorithm implementation with I-V curve-adjusting R_s and R_p and P-V curve-adjusting peak power respectively and figures 2.14 and 2.15 shows the adjusted curves after Parameter estimation algorithm implementation respectively.

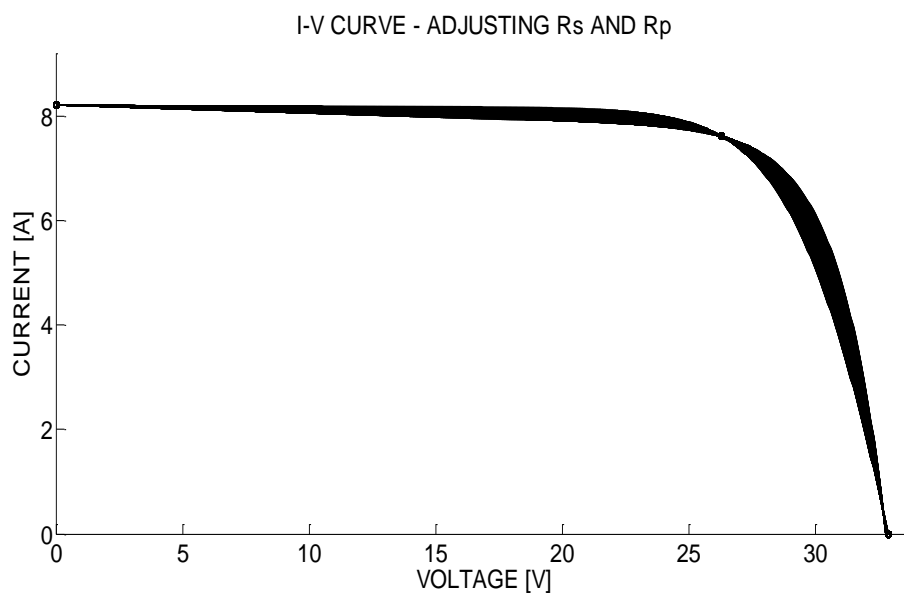


Figure 2.12: I-V curve - adjusting R_s and R_p

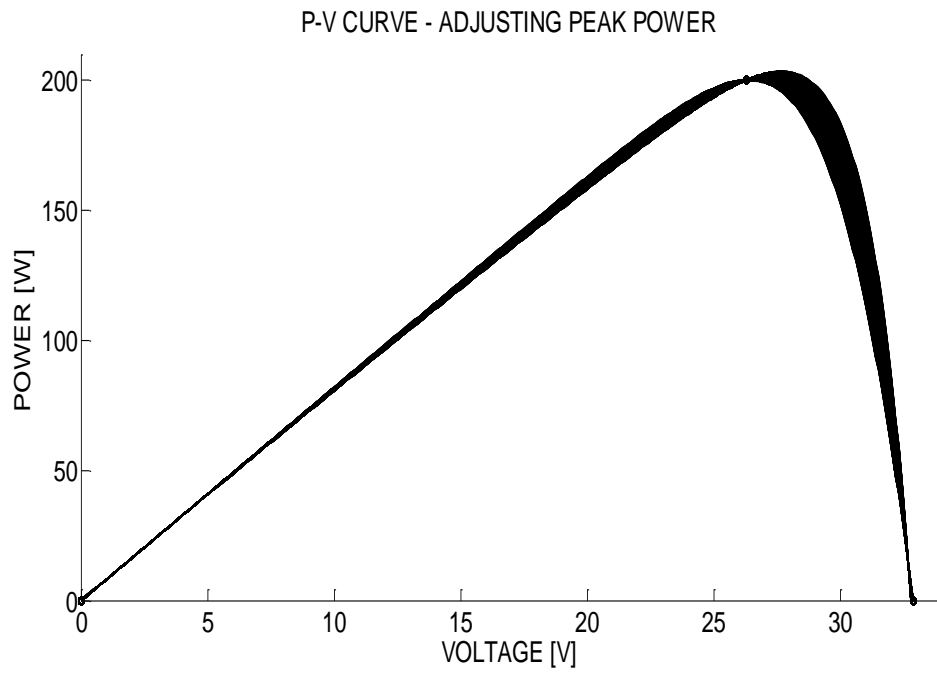


Figure 2.13: P-V curve - adjusting peak power

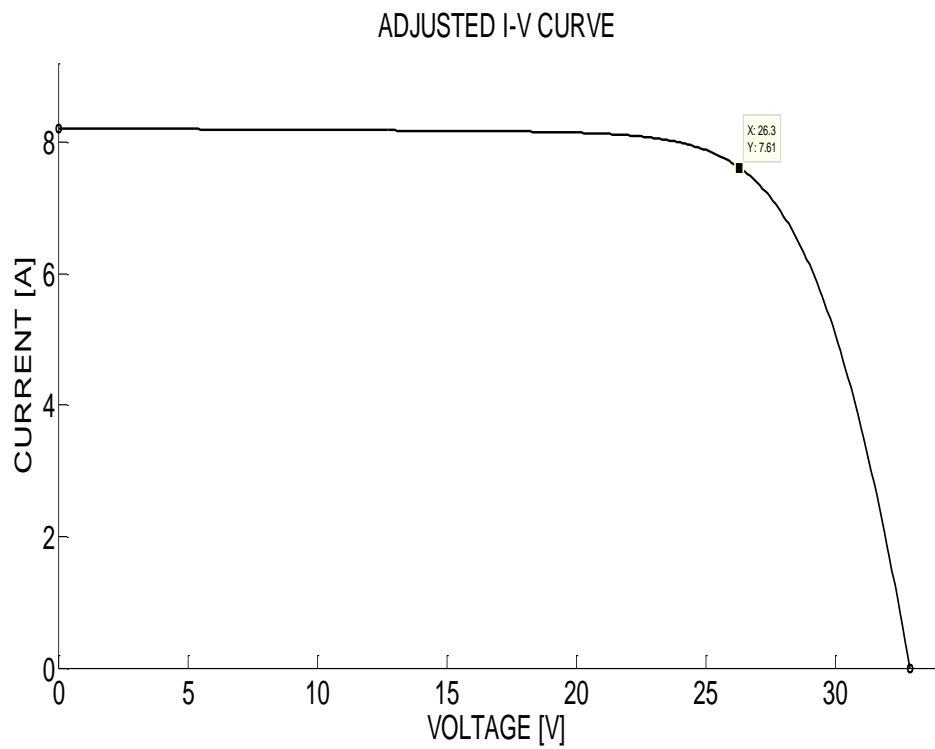


Figure 2.14: Adjusted I-V curve

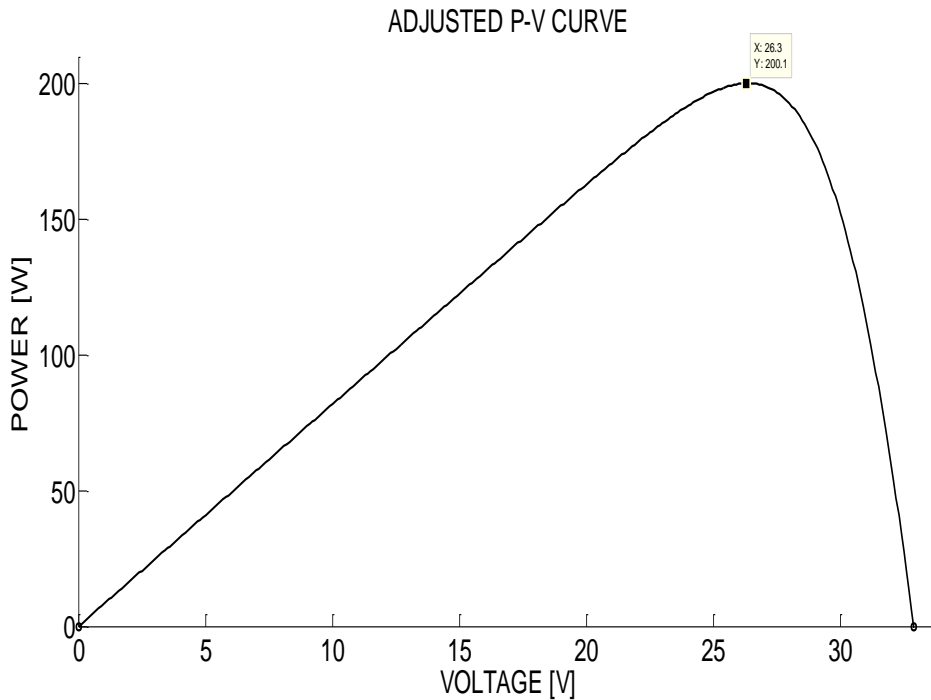


Figure 2.15: Adjusted P-V curve

2.73 Simulink Model of PV Array

A single diode model with R_s and R_p is implemented in MATLAB/ SIMULINK. Here, a panel of 200 W is selected and grouped such that $N_{ser} = 15$ and $N_{par} = 2$, therefore $P_{max} = 6000$ ($15 \cdot 2 \cdot 200$) W. The 6 kW PV array is as shown in figures 2.16 through 2.20.

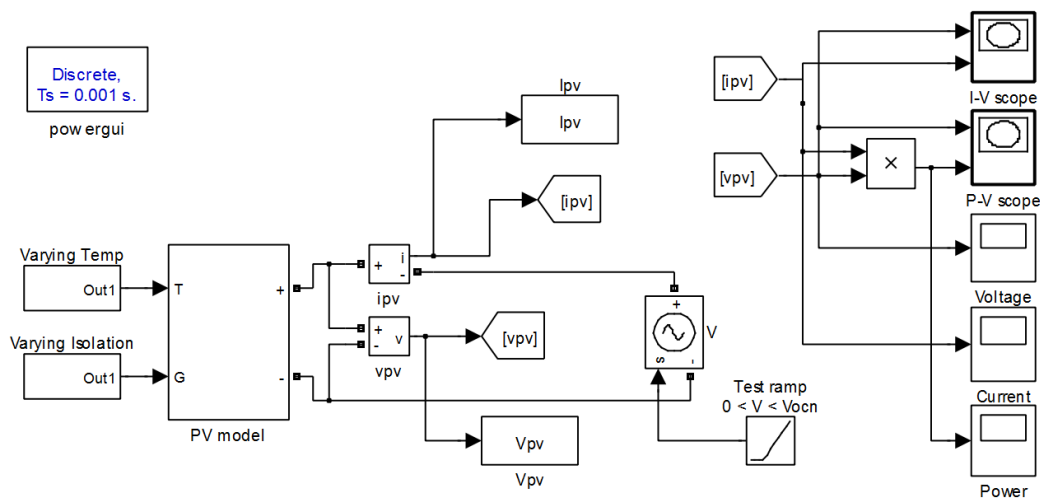


Figure 2.16: Simulink PV array model

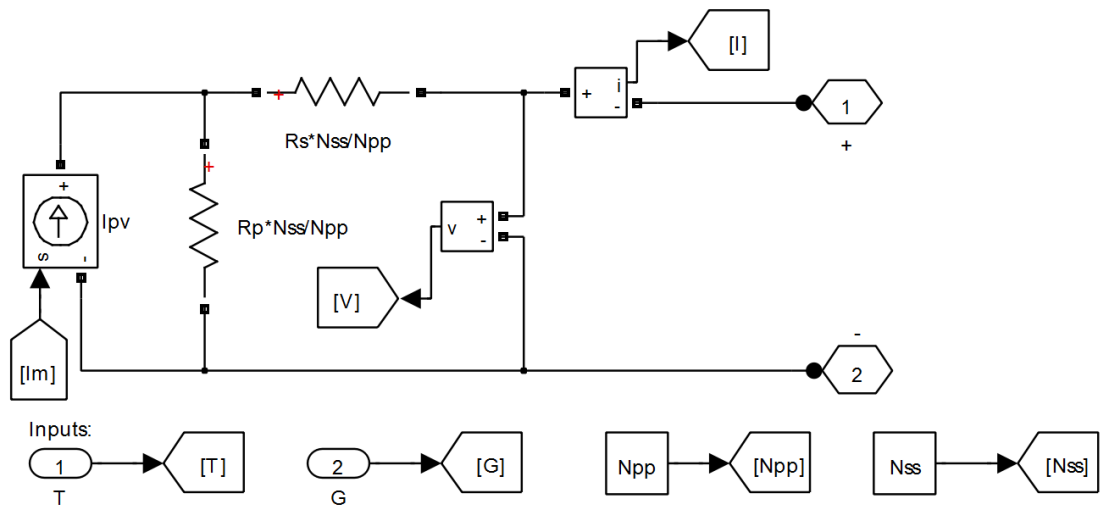


Figure 2.17: PV model subsystem

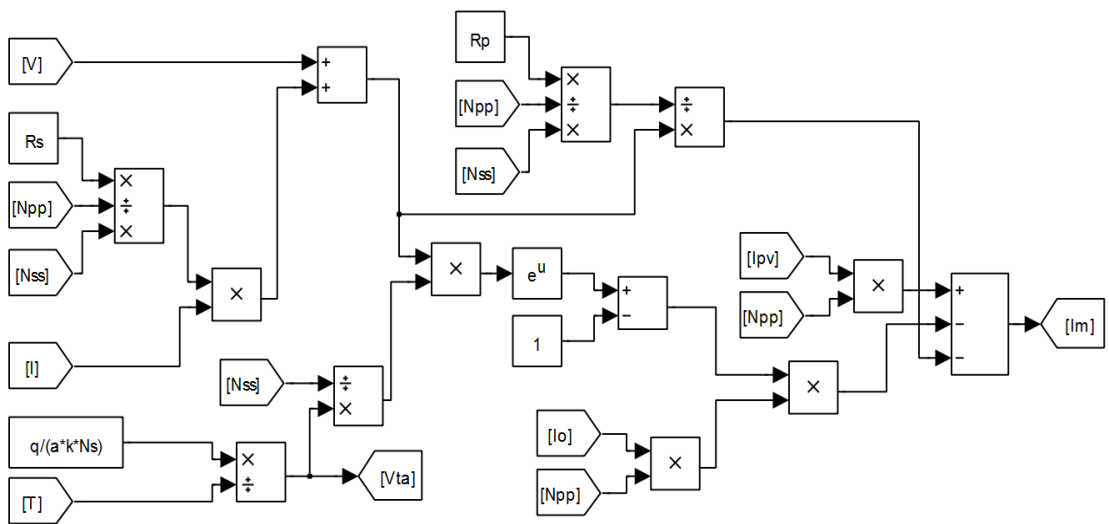


Figure 2.18: Calculation of Im

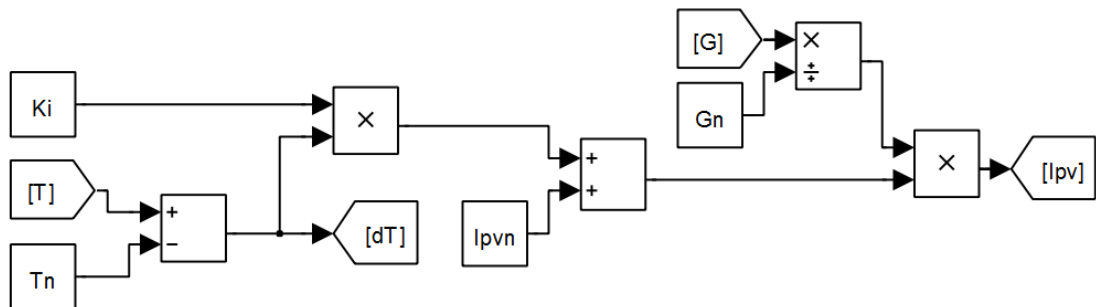


Figure 2.19: Calculation of Ipv

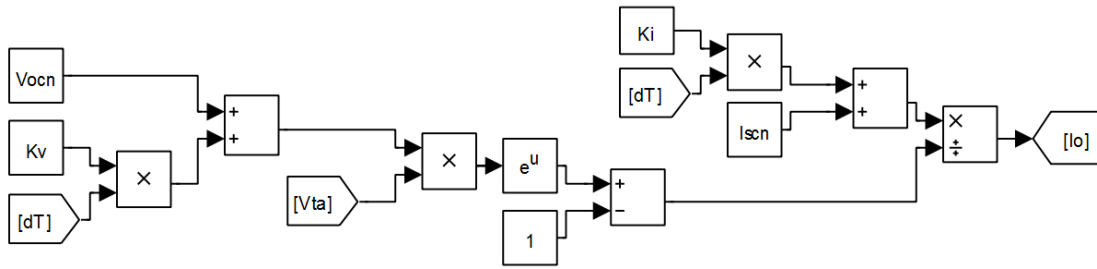


Figure 2.20: Calculation of I_0

The working of the PV model for various Temperature changes at a constant irradiance of 1000 W/m^2 is shown in the figures 2.21 and 2.22.

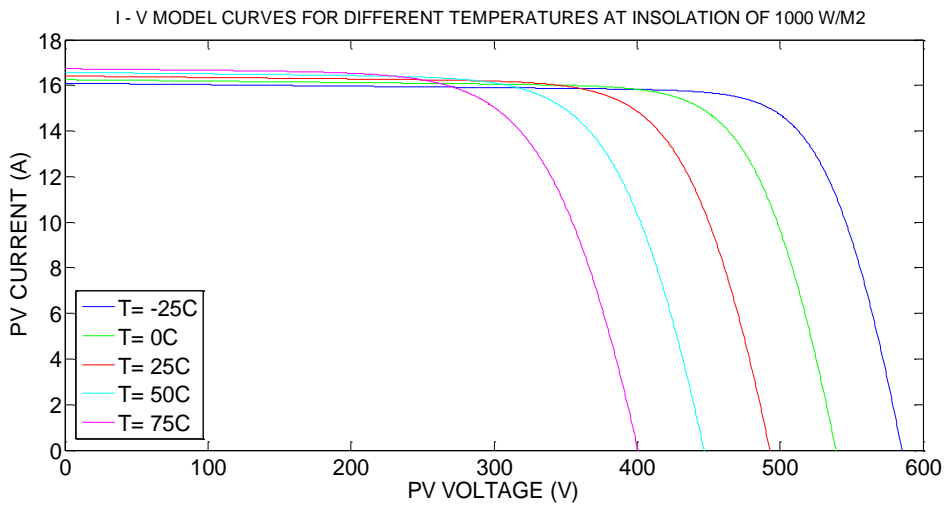


Figure 2.21: I-V model curves for different temperatures

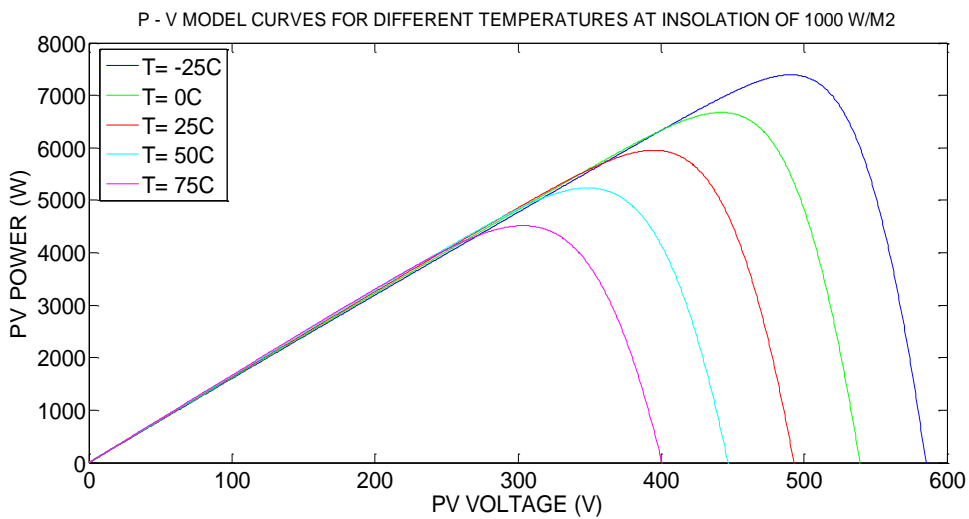


Figure 2.22: P-V model curves for different temperatures.

Thus, the PV module variations with temperature are observed. As the temperature increases, the voltage and power decreases while the current is almost same. And vice versa i.e. as the temperature decreases, the voltage and power increases while the current is almost same.

The working of the PV model for various irradiance changes at a constant temperature of 25°C is as shown in the figures 2.23 and 2.24.

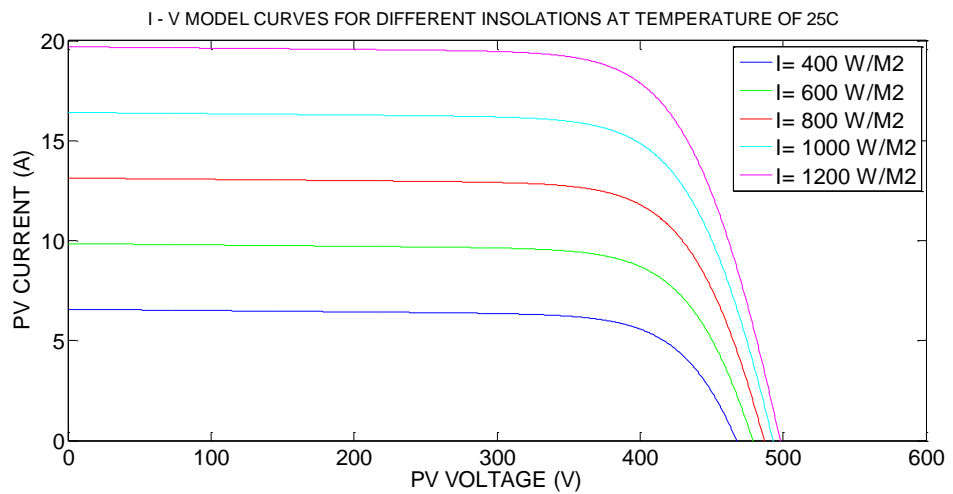


Figure 2.23: Model I-V curves for different irradiances

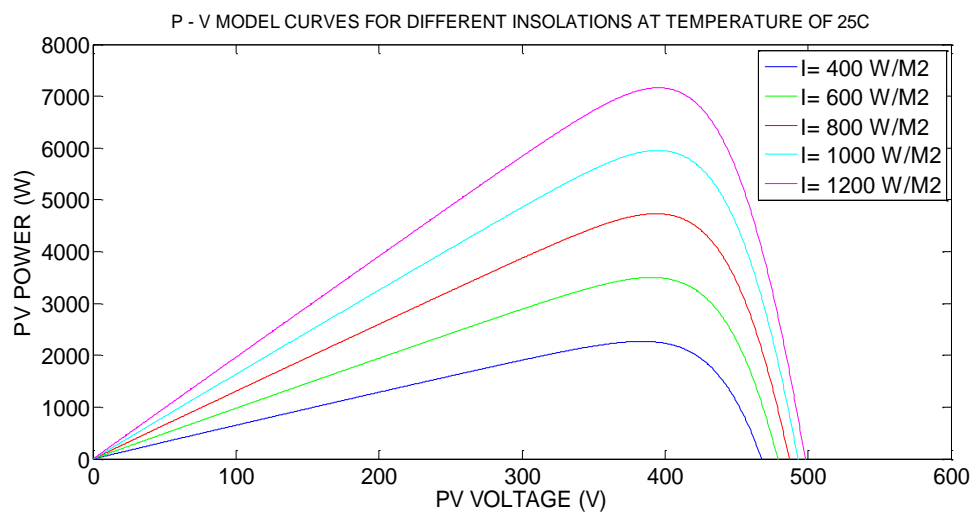


Figure 2.24: P-V model curves for different irradiances

Here as the irradiance increases, the current and power increases but the voltage remains almost the same and vice versa.

2.74 PV Model with MPPT

The PV array is connected to the R load, through a DC-DC boost converter. The PV array system implemented in simulink is as shown in the figure 2.25.

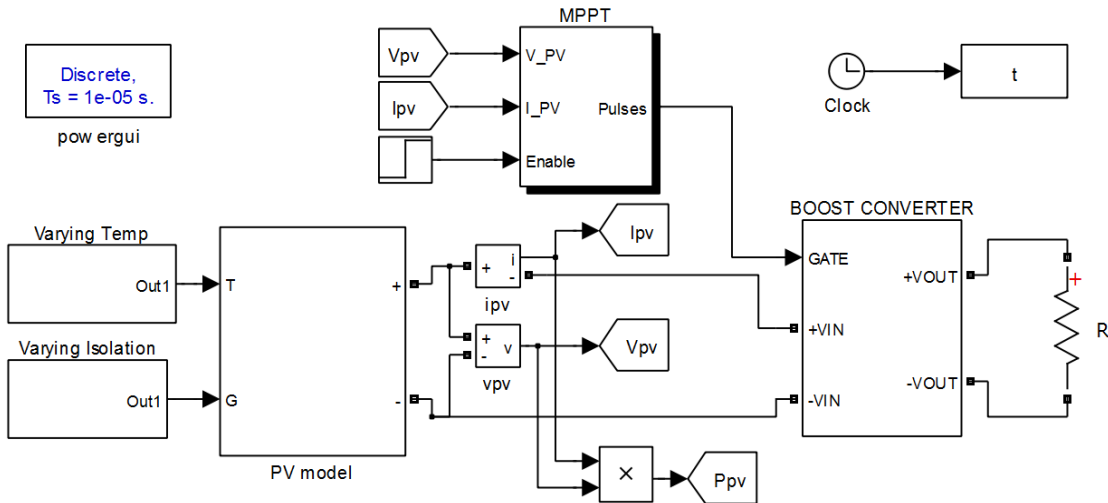


Figure 2.25: Simulink PV system model.

The Incremental conductane method is applied as MPPT. The MPPT block gives the duty cycle at which the boost converter should operate. The incremental conductance is implemented with a PI control and error margin of ± 0.02 . The MPPT subsystem is implented in simulink as shown in figures 2.26 and 2.27.

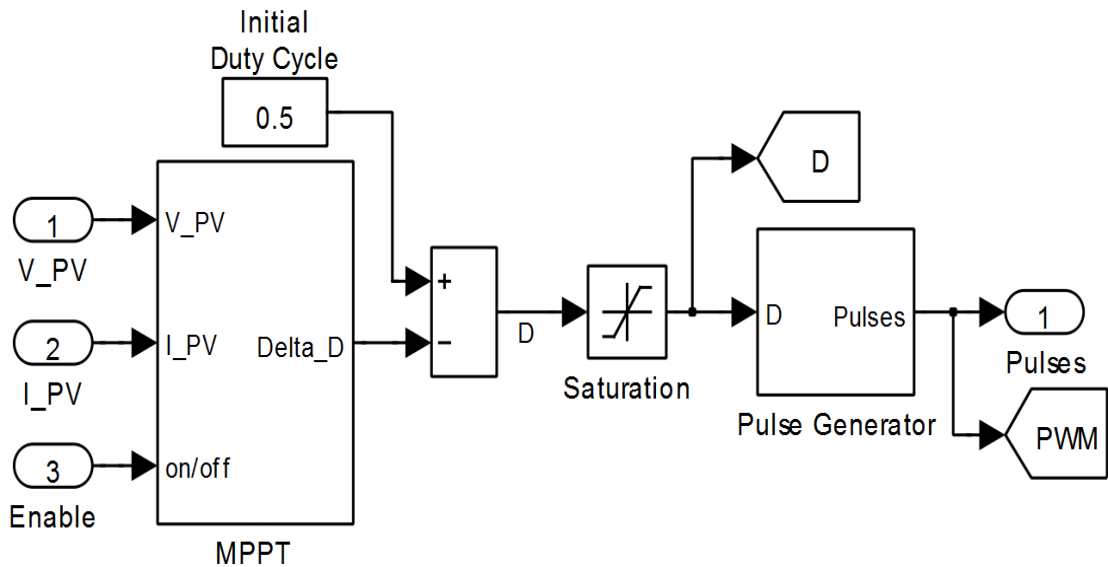


Figure 2.26: MPPT subsystem

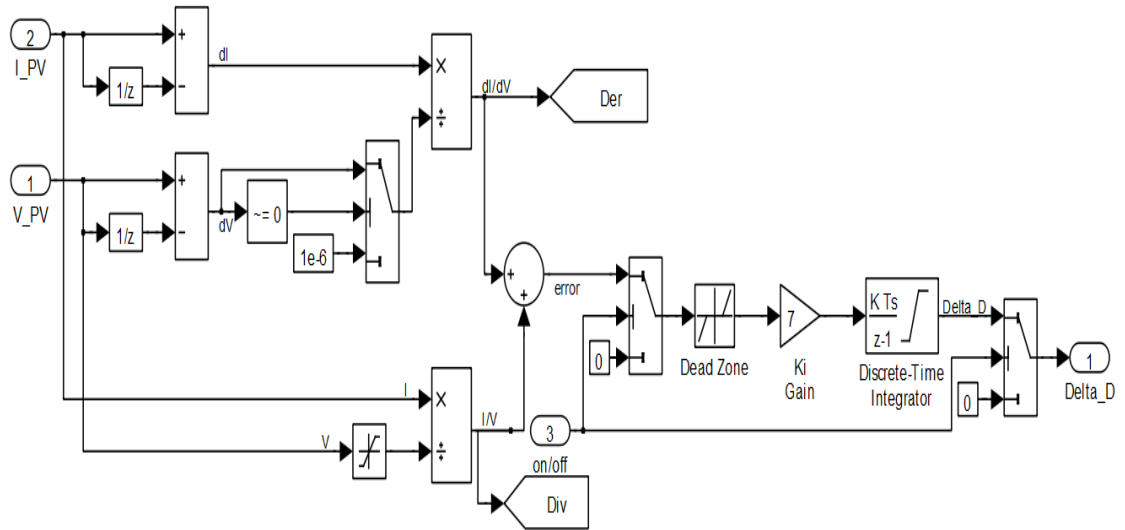


Figure 2.27: Simulink model of Inc Cond

The boost converter is designed with the specifications in Table 2.3.

Table 2.3: Boost converter specifications.

V_i	394.5
V_o	700 V
P_o	6000 W
F_s	10 KHz
ΔI_o	20 %
ΔV_o	5 %

The inductance (L) in the converter is taken as $7e-3$, the capacitance (C) is taken as $50e-6$, and capacitance (C1) is taken as $5000e-6$. The switch used is IGBT. The boost converter implementation in simulink is shown in figure 2.28.

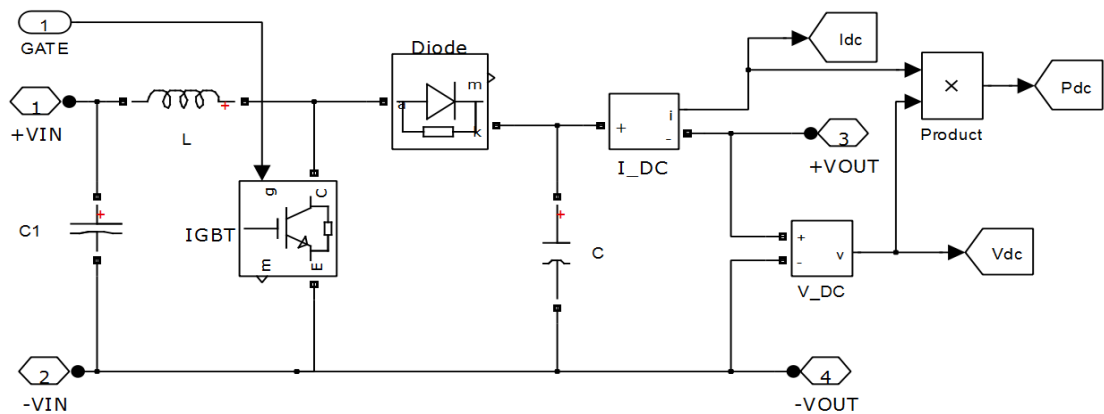


Figure 2.28: Boost converter implemented in simulink

The temperature is varied from 25°C - 45°C in steps of 5°C for every 2 seconds and irradiation is varied from 400 – 800 W/m² in steps of 100 W/m² for every 2 seconds. The variations are as shown in figure 2.29.

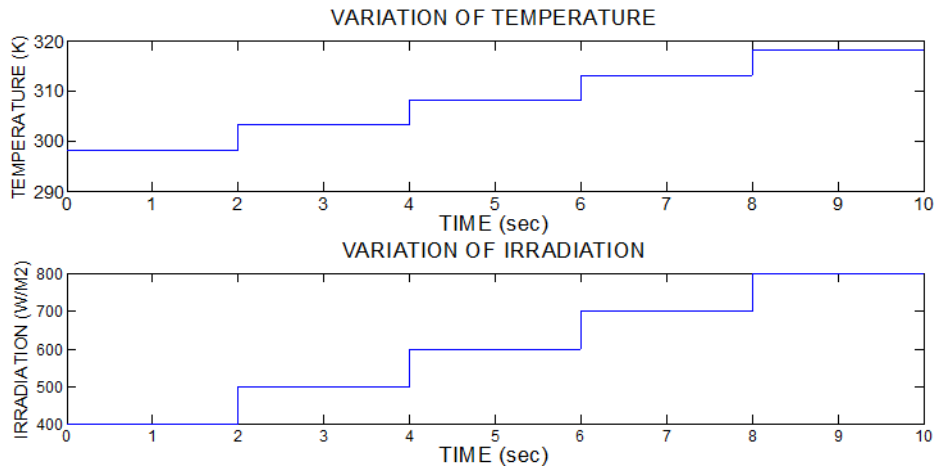


Figure 2.29: Temperature and Irradiation variations

The MPPT tracks the maximum power point with nearly 98 % effectiveness even for varying changes in temperature and irradiation. The tracking ability of the MPPT for various changes in temperature and irradiation are as shown in figure 2.30.

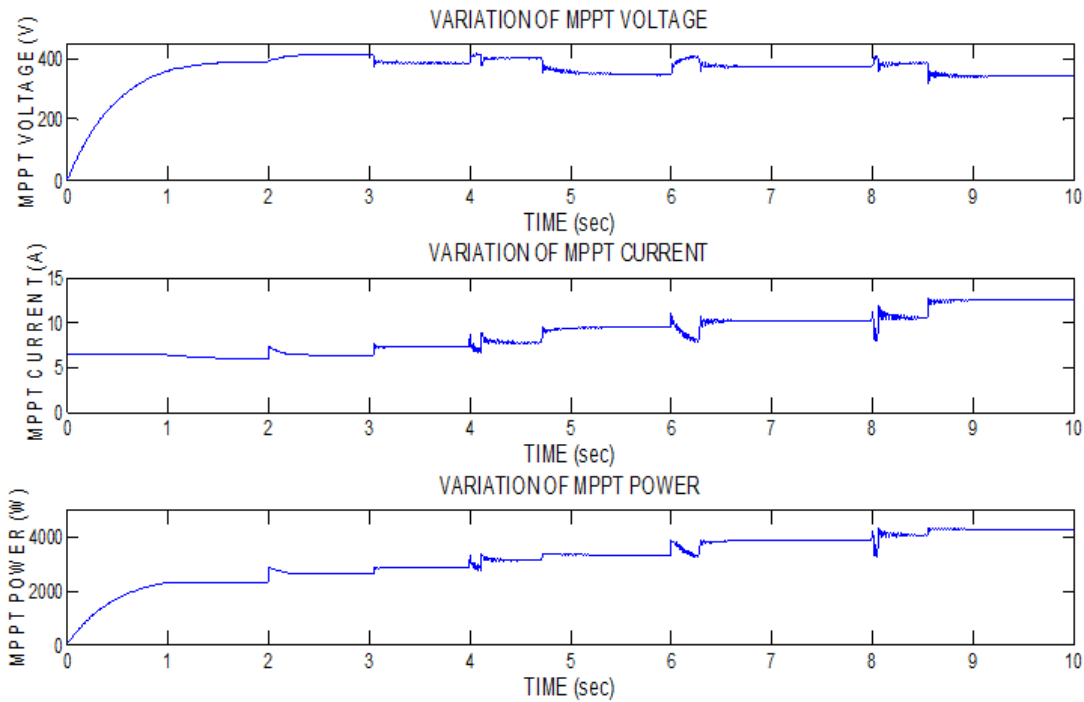


Figure 2.30: waveforms of the MPP voltage, current and power

The boost converter outputs the power with an efficiency of nearly 92 %.

CHAPTER 3

MICRO TURBINE

The small DG systems based on micro turbine technology are gaining popularity amongst industry and utilities in the last few years due to following salient features:

- Relatively small in size among other DGs.
- High efficiency, fuel-to-electricity conversion can reach 25- 30%.
- They are environmentally superior
- Durable, designed for 11,000 hours of operation between major overhauls, and a service life of at least 45,000 hours.
- They are economical with system costs lower than \$500 per kilowatt
- Fuel flexibility they can use alternative/optional fuels including natural gas, diesel, ethanol, landfill gas, and other biomass-derived liquids and gases.

The Micro Turbine Generator (MTG) system generates power in the range of 25 kW to 500 kW and can be operated in standalone, mobile, remote or interconnected with the utility applications.

3.1 Types of Micro Turbine Systems

There are mainly two types of micro turbine systems available, single-shaft models and split shaft models. In single-shaft designs, a single expansion turbine turns both the compressor and the generator. In single-shaft design, a single expansion turbine turns both the compressor and the generator. As a result it operates at high-speeds, some in excess of 100,000 rpm, and generate electrical power at high frequency (in the order of kHz). (D. N. Gaonkar et al. 2011,). The Single shaft Micro Turbine and Split shaft Micro turbine are as shown in figure 3.1 and 3.2.

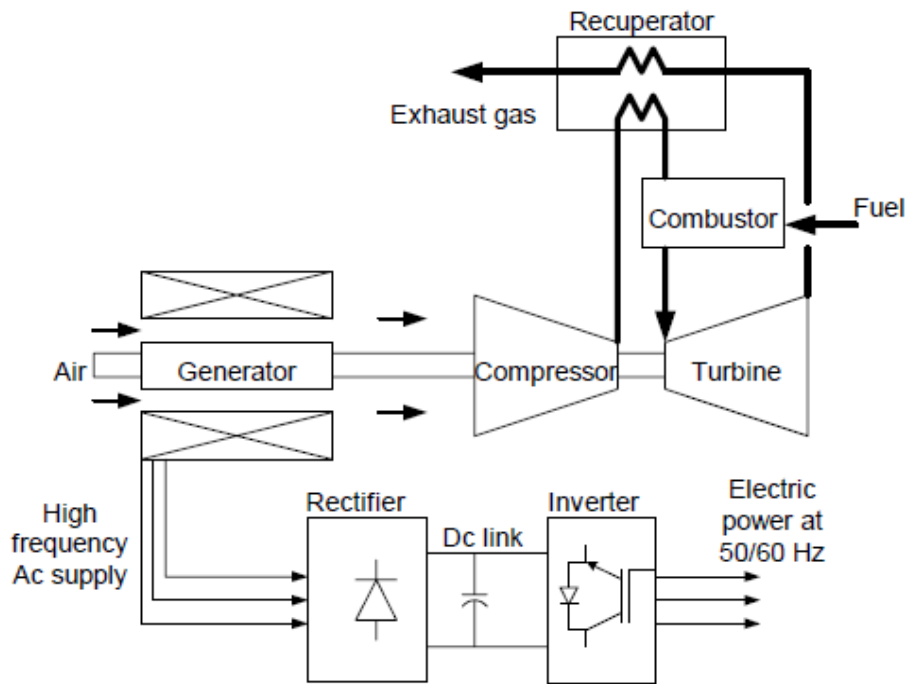


Figure 3.1: Single shaft Micro Turbine

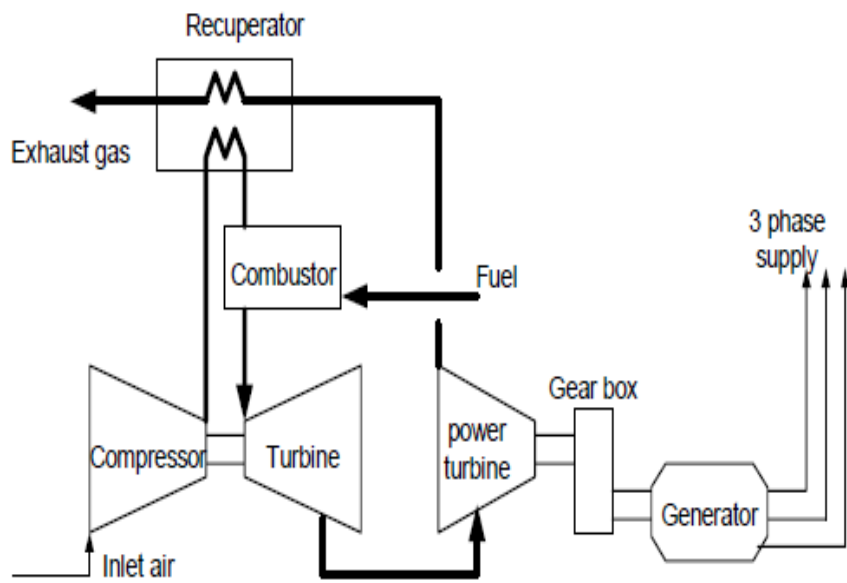


Figure 3.2: Split shaft Micro turbine

3.2 Modeling of MTG

The concept of gas turbine system presented in this section is based on the paper by Rowen. It is a proposal with single-shaft design, generator driven gas turbine model which includes speed control, temperature control and fuel system.

The model used in this work focuses on the slow dynamics of the MTG system for power management of MTG combined with other DG systems.

The figure 3.3 shows the per-unit representation of a micro turbine, along with its control systems.

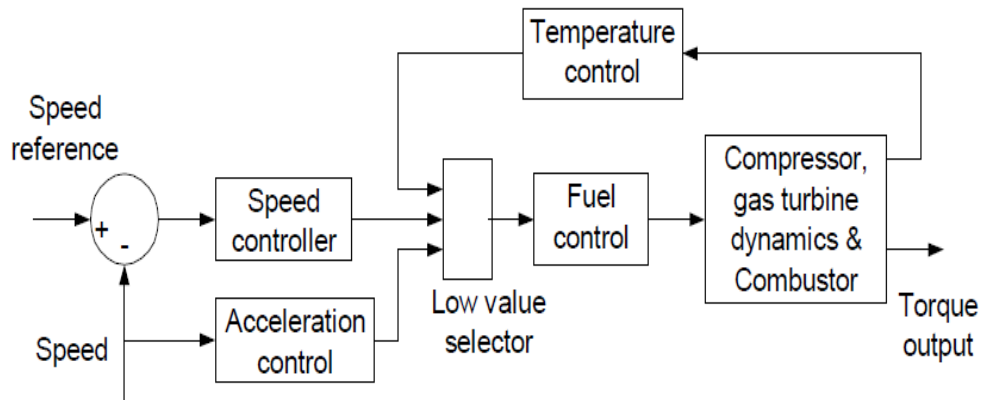


Figure 3.3: Block diagram of a micro turbine

3.2.1 Speed and Acceleration Control

The speed control operates on the speed error formed between a reference (one per-unit) speed and the MTG system rotor speed. In this work, a lead lag transfer function has been used to represent the speed controller as shown in figure 3.4.

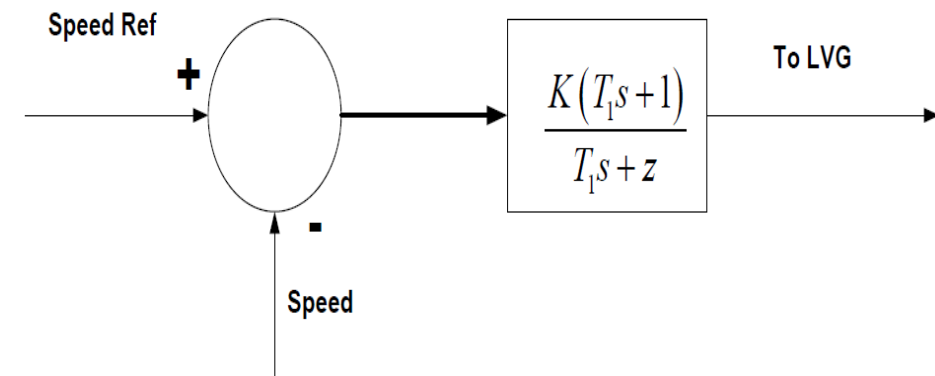


Figure 3.4: Speed Control

3.2.2 Fuel Control

The fuel system consists of the fuel valve and actuator.

The fuel flow control is as shown in figure 3.5.

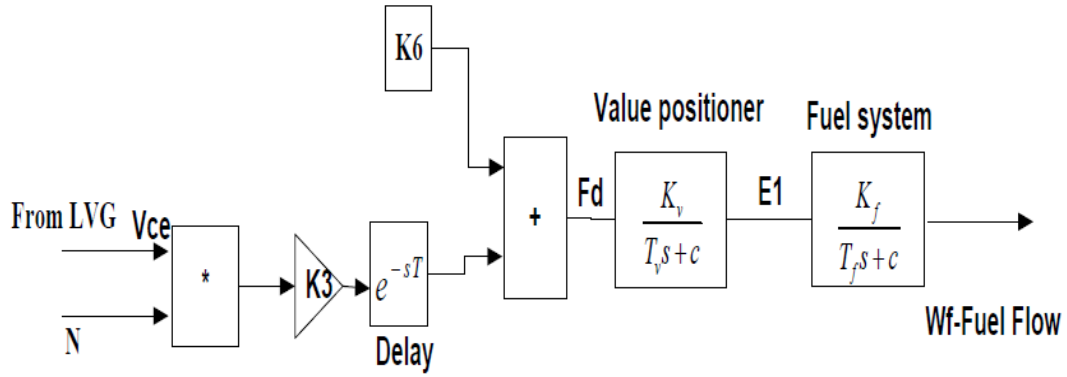


Fig 3.5: Fuel Control system

The valve positioner transfer function is as shown in equation 3.1.

$$\frac{E_1}{F_d} = \frac{K_v}{T_v s + C} \quad (3.1)$$

and the fuel system actuator transfer function is as shown in equation 3.2.

$$\frac{W_f}{E_1} = \frac{K_f}{T_f s + C} \quad (3.2)$$

3.2.3 Compressor and Turbine

The compressor-turbine is essentially a linear, non-dynamic device. The block diagram of the compressor-turbine package is as shown in figure 3.6.

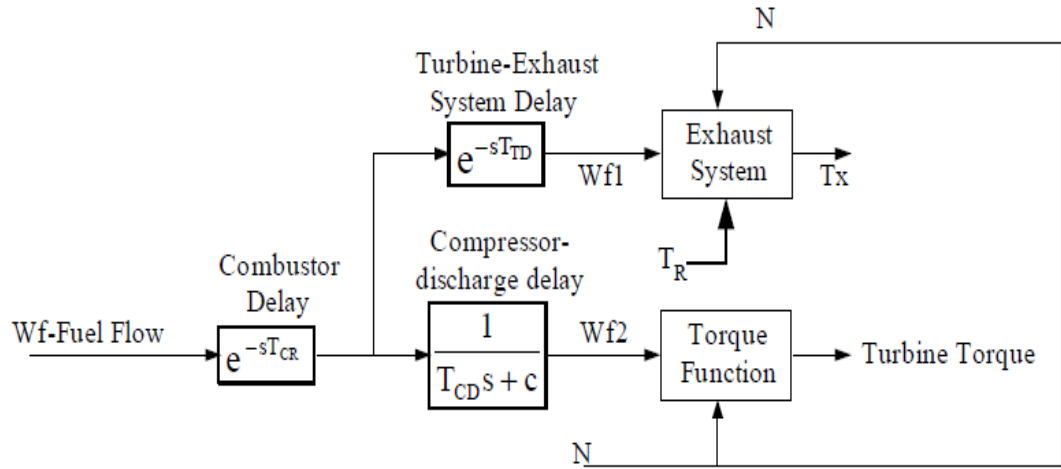


Figure 3.6: Compressor and Turbine system

The torque and the exhaust temperature characteristics of the single-shaft gas turbine are given by the following equations 3.3 and 3.4 respectively.

$$Torque = K_{HHV}(W_{f2} - 0.23) + 0.5(1 - N) \quad (3.3)$$

$$Exhaust Temp, T_x = T_R - 700(1 - W_{f1}) + 550(1 - N) \quad (3.4)$$

3.2.4 Temperature Control

The block diagram of the temperature controller is as shown in the Figure 3.7

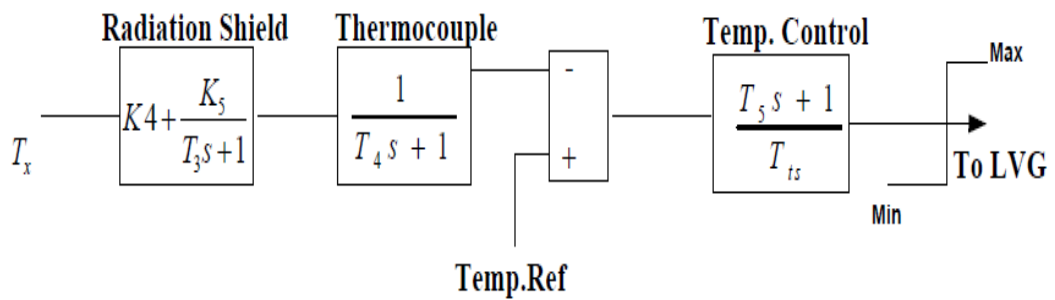


Figure 3.7: Temperature Control system

3.3 Permanent Magnet Synchronous Generator (PMSG)

The mathematical model of a PMSG is similar to that of the wound rotor synchronous machine. Few assumptions are made in the modelling such as Saturation is neglected.

The stator dq-axis equivalent circuits of the PMSG are as shown in the figures 3.8.

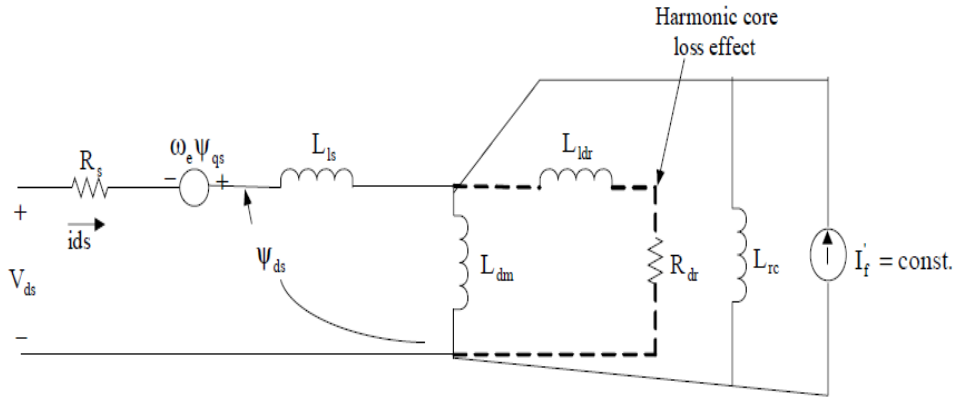


Figure 3.8: d axis equivalent circuit

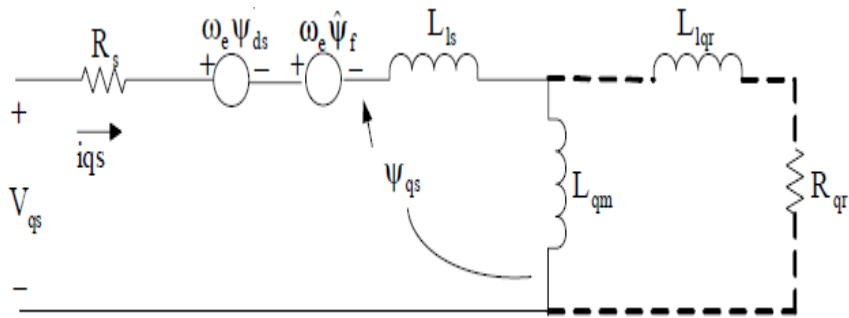


Figure 3.9: q axis equivalent circuit

With the assumptions the stator dq equations are as given in equations below. The Electrical equations are as shown in equation 3.5, 3.6, 3.7.

$$\frac{dI_d}{dt} = \frac{V_d}{L_d} - \frac{RI_d}{L_d} + \frac{L_q}{L_d} p w_r I_q \quad (3.5)$$

$$\frac{dI_q}{dt} = \frac{V_q}{L_q} - \frac{RI_q}{L_q} - \frac{L_d}{L_q} p w_r I_d - \frac{\lambda p w_r}{L_q} \quad (3.6)$$

$$T_e = 1.5p(\lambda I_q + (L_d - L_q)I_d I_q) \quad (3.7)$$

The mechanical equations are as shown in equation 3.8 and 3.9.

:

$$\frac{dw_r}{dt} = \frac{1}{J} (T_e - F w_r - T_m) \quad (3.8)$$

$$\frac{d\theta}{dt} = w_r \quad (3.9)$$

3.4 Power Conditioning System

The power conditioning is a critical component in the single-shaft micro turbine design and represents significant design challenges, specifically in matching turbine output to the required load. Power conditioning unit consists of a three phase diode rectifier, a voltage source inverter (VSI) and LC filter.

3.4.1 Three Phase Diode Bridge Rectifier

Three-phase bridge rectifiers are commonly used for high power applications. The circuit of a three-phase bridge rectifier is as shown in figure 3.10.

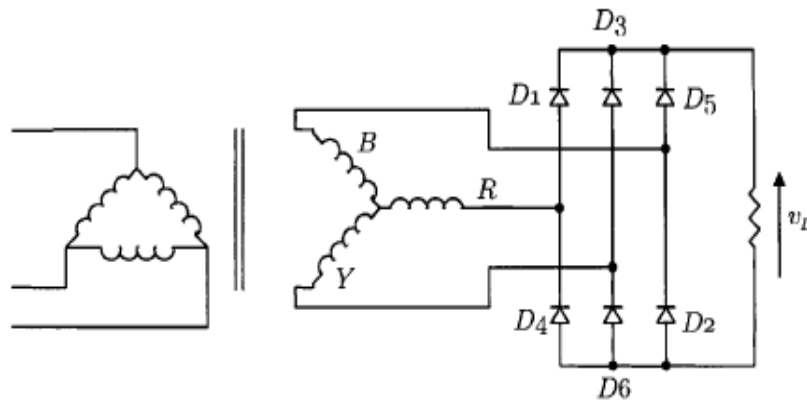


Figure 3.10: 3 Phase diode bridge rectifier

The voltage and current waveforms of the three-phase bridge rectifier are shown in figure 3.11.

The average value of the output voltage is as shown in equation 3.10.

$$V_{dc} = \frac{3\sqrt{3}V_m}{\pi} \quad (3.10)$$

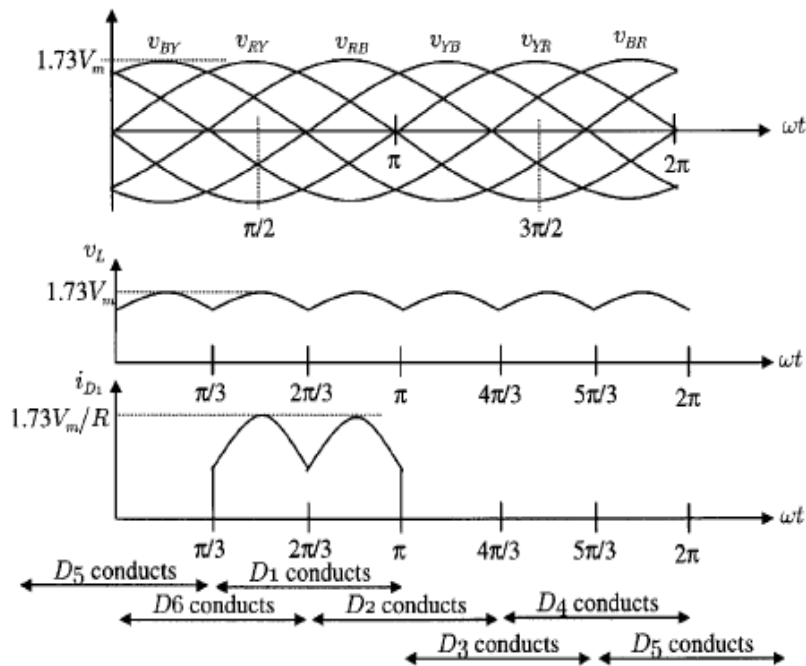


Figure 3.11: 3 Phase diode bridge rectifier waveforms

3.4.2 Three Phase PWM Inverter

The inverter is used to convert the DC to AC, so it is DC- AC Converter. A sinusoidal pulse width modulation (SPWM) controller was used to control the inverter in order to meet the voltage regulation. The power electronics interface used has the ability to control the load voltage by using the PI voltage regulator using abc to dq and dq to abc transformation. The output of the voltage regulator is a vector containing the three modulating signals used by the PMW generator to generate the gate pulses. The three phase inverter is shown in the figure 3.12.

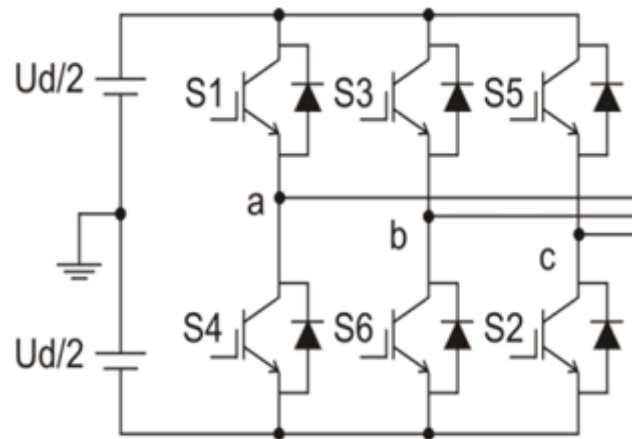


Figure 3.12: Three phase inverter

3.4.2.1 VF Control

In general, there are three ways to regulate the voltage of the inverter and are:

- PQ control
- PV control
- VF control

Since this is in standalone mode, VF control is being used. PQ and PV control are used in grid connected modes. The VF control is done as shown 3.13.

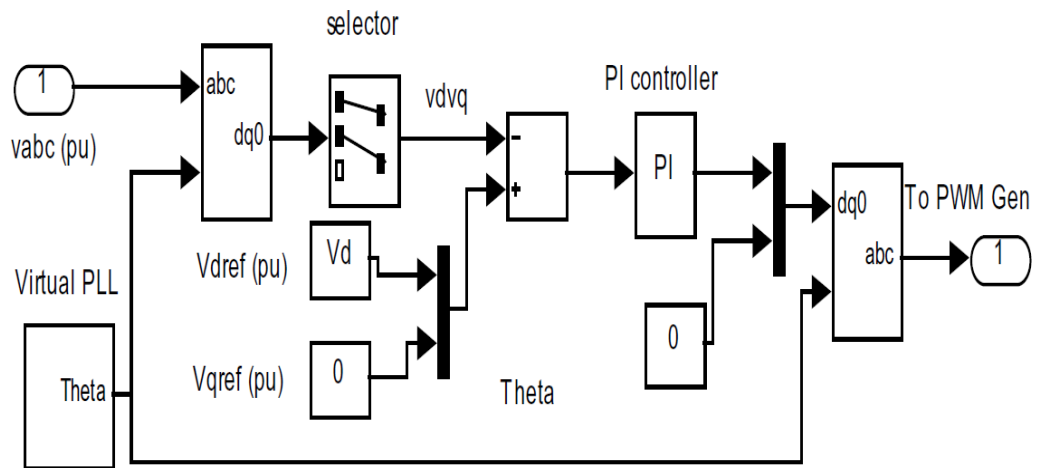


Figure 3.13: VF control system

3.4.2.2 Sinusoidal Pulse Width Modulation

In the most straightforward implementation, generation of the desired output voltage is achieved by comparing the desired reference waveform (modulating signal) with a high frequency triangular ‘carrier’ wave as depicted schematically in figure 3.14.

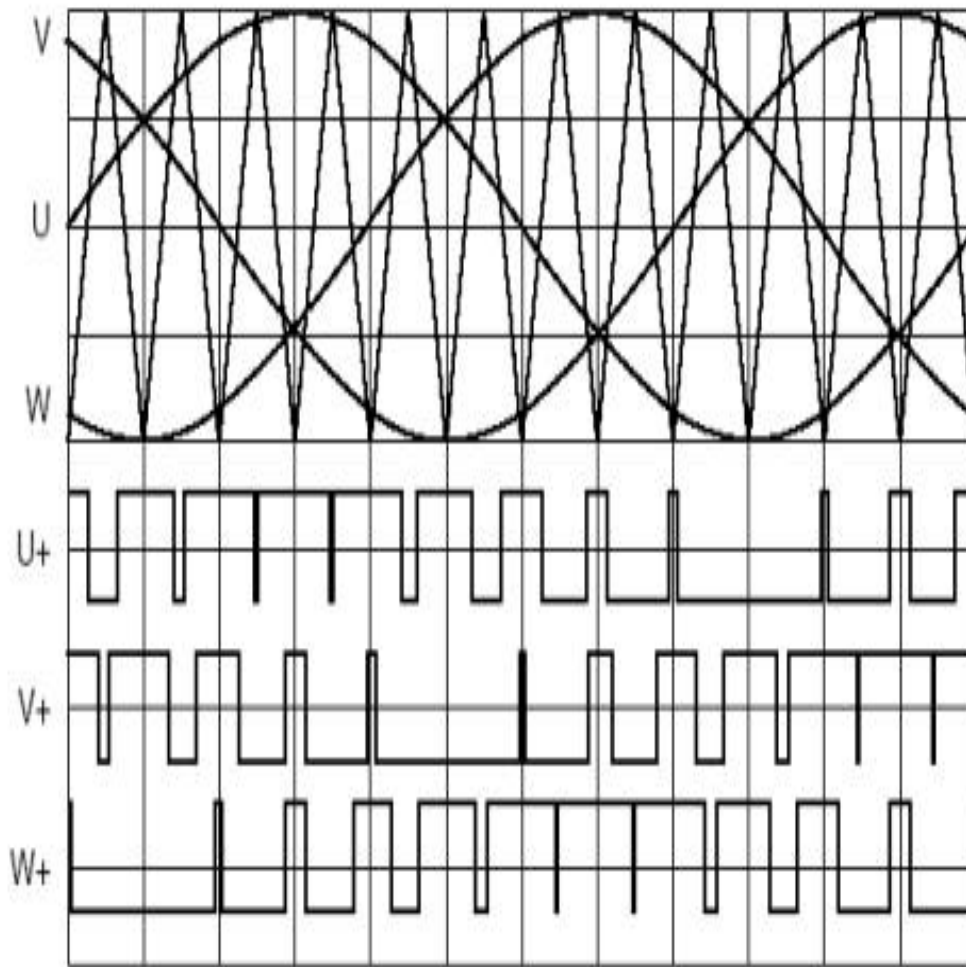


Figure 3.14: Sinusoidal pulse width modulation

In three-phase systems, it is advisable to use frequency modulation as shown in equation 3.11 (Muhammad H. Rashid 2001).

$$m_f = \frac{f_c}{f_m} = 3K \quad (K \in N) \quad (3.11)$$

And that all three waveforms are symmetric and there are no even harmonics as well as triplen harmonics.

3.5 Filter

The harmonics generated by the inverter are around multiples of switching frequency and are filtered by the LC low pass filter. The corner frequency of the LC filter has to be chosen to filter the PWM switching ripples of the inverter and pass the fundamental frequency component without attenuation. The LC low pass filter is used for eliminating the higher order harmonics and only allowing the fundamental frequency component. The figure 3.15 shows the LC low pass filter.

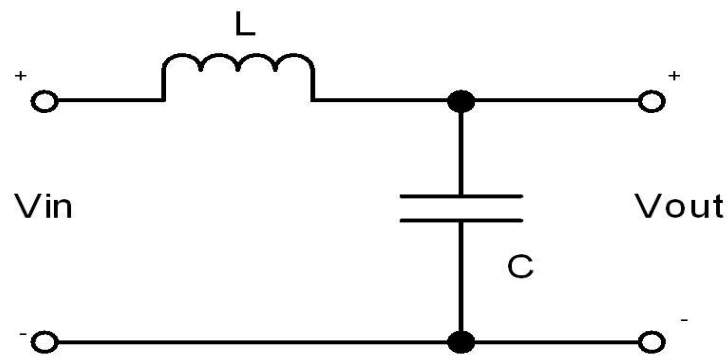


Figure 3.15: LC low pass filter

The frequency response of the LC low pass filter is as shown in figure 3.16.

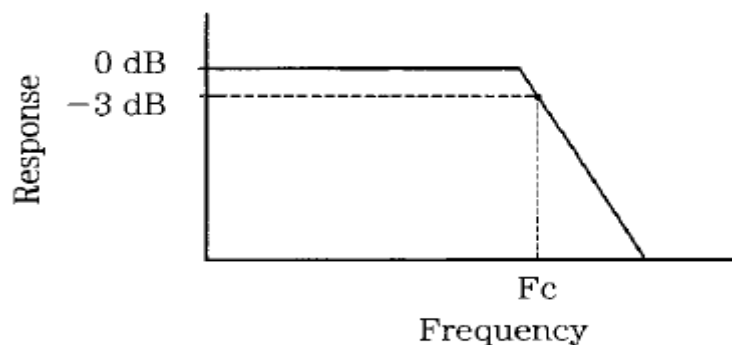


Figure 3.16: Frequency response of LC low pass filter

The corner frequency of the filter is as shown in equation 3.12.

$$F_c = \frac{1}{2\pi\sqrt{LC}} \quad (3.12)$$

3.6 Simulation results

In micro turbine system, the micro turbine model is connected to a PMSG. The PMSG output is connected to a 3 phase diode bridge rectifier for converting the high frequency AC to DC. A 3 phase SPWM inverter is used for converting the DC to AC of frequency 50 Hz. The VF control is used for the voltage control of inverter. The load is varied from 15 kW at $t=0$ to 18 kW at $t=5$ and to 21kW at $t=10$. The RMS value of the voltage is 440 V. The Micro turbine system implemented in SIMULINK is as shown in figure 3.17.

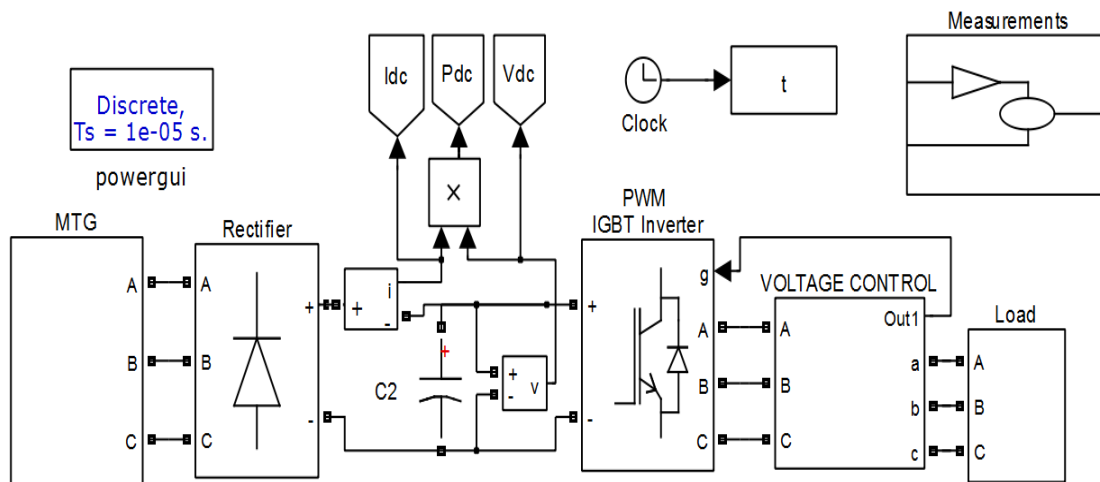


Figure 3.17: Micro turbine system

The Microturbine generator subsystem and micro turbine subsystem are shown in the figures 3.18 and 3.19 respectively. The acceleration control and temperature control are not considered in the design.

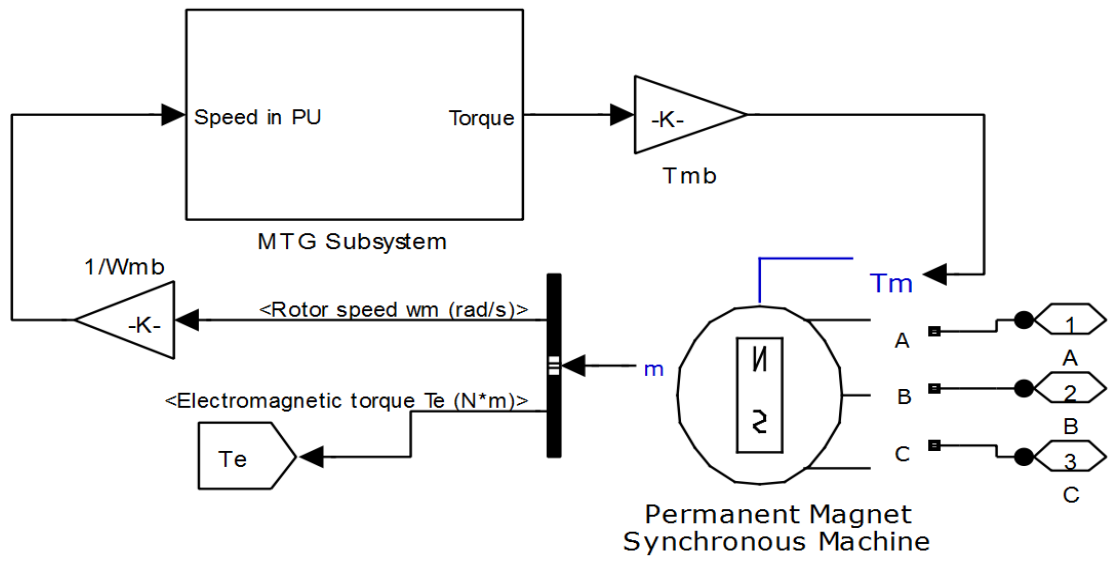


Figure 3.18: Micro turbine generator subsystem

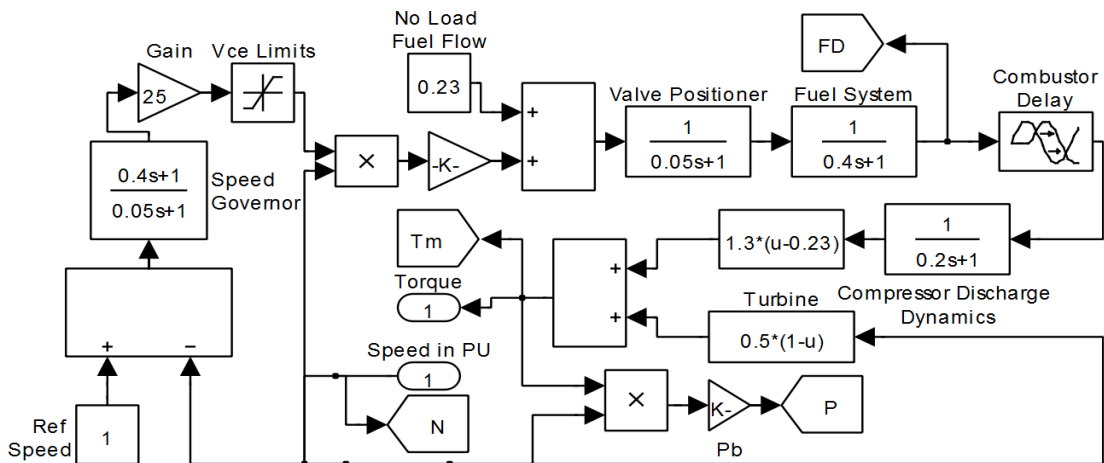


Figure 3.19: Micro turbine subsystem

The voltage control subsystem is shown in figure 3.20 and Speed, torque and MTG power are as shown in figure 3.21.

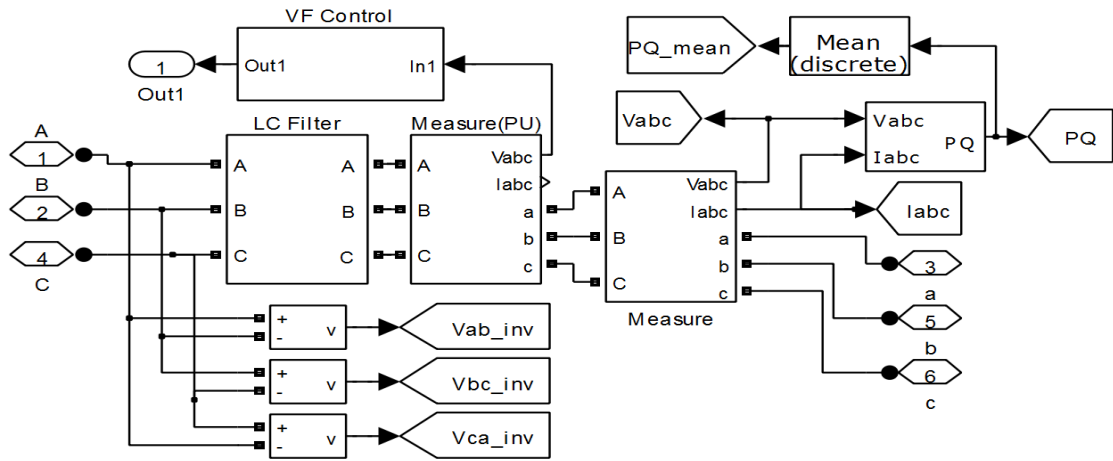


Figure 3.20: Voltage control subsystem

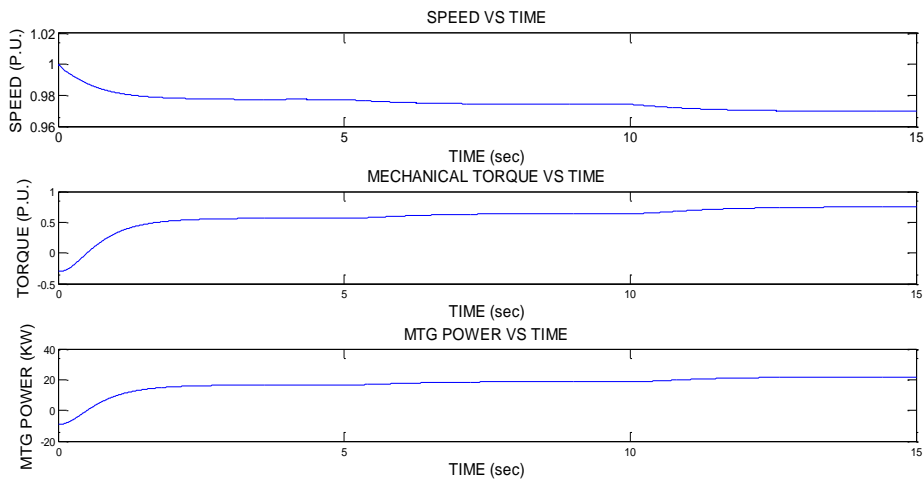


Figure 3.21: Speed, Torque and Power of Micro turbine

The DC link voltage, current and power curves are shown in figure 3.22.

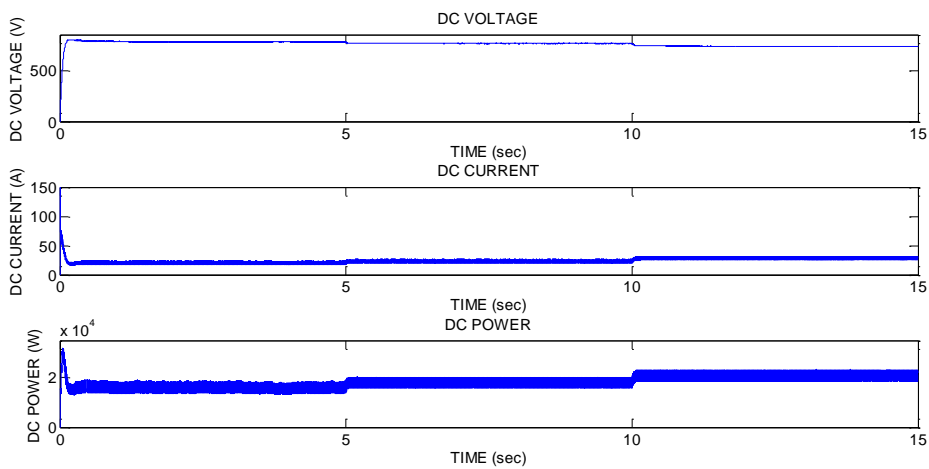


Figure 3.22: DC link voltage,current and power

The inverter and load waveforms are shown in figure 3.23 and 3.24 respectively.

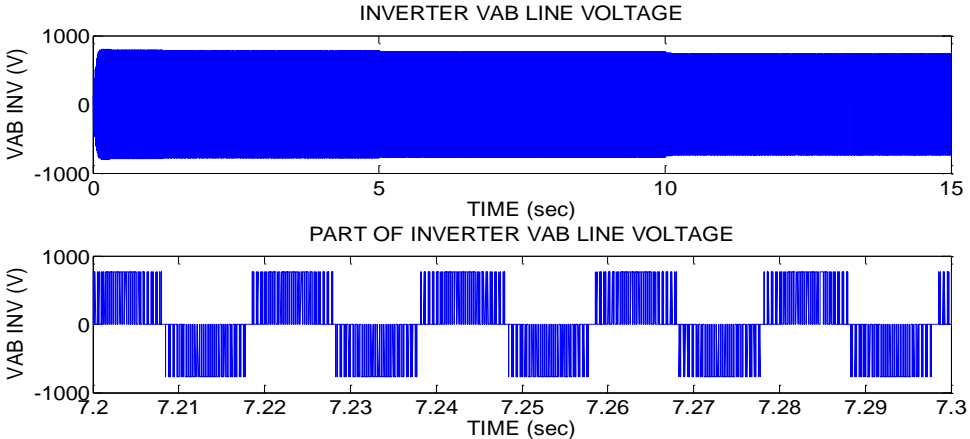


Figure 3.23: Inverter V_{ab} line voltage

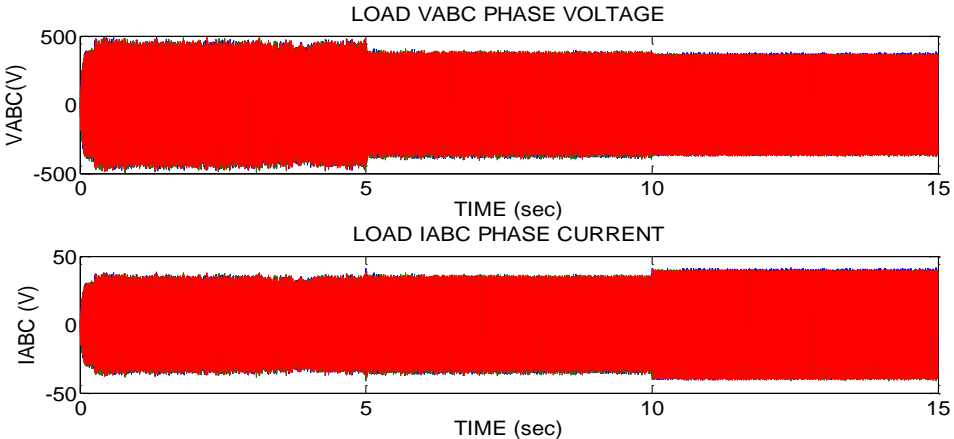


Figure 3.24: Load phase current and voltage waveforms

The load phase voltage and current for a one second is as shown in figure 3.25.

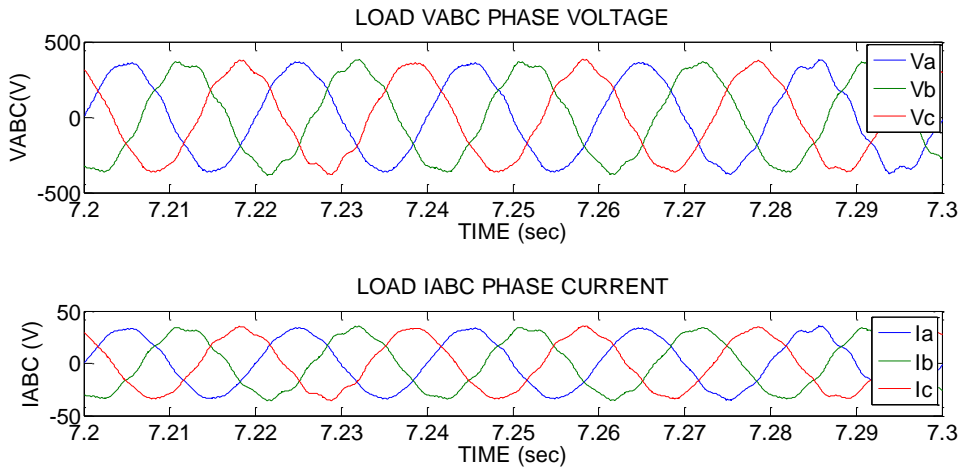


Figure 3.25: Part of load phase voltage and current waveforms

The load power (P and Q) are as shown in figure 3.26.

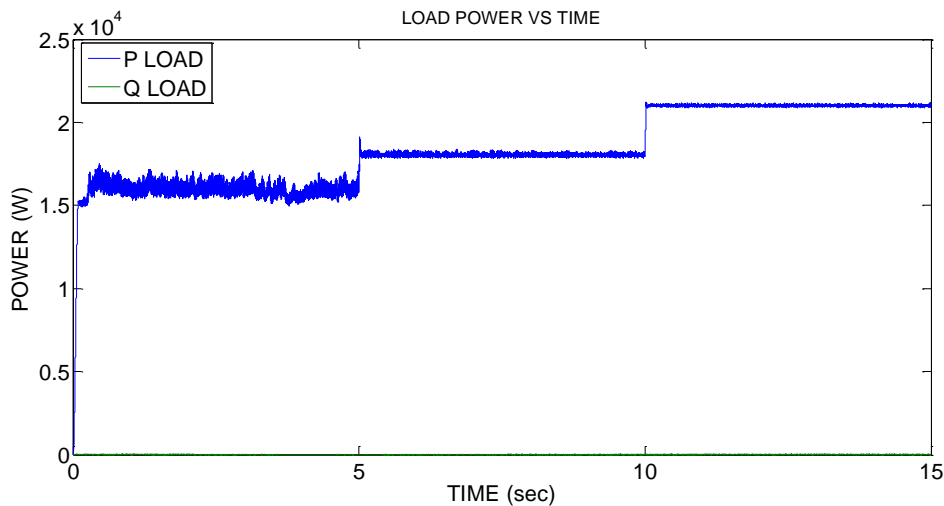


Figure 3.26: Load power

Thus, it clearly shows that the MTG system is operating to match the load requirements. The speed initially at 1 p.u. drops to 0.9773 for 15 kW, 0.9743 for 18 kW and 0.9697 for 21 kW. The mechanical torque increases from 0.565 to 0.643 and to 0.75 for same load changes. The DC link voltage drops from 780 V at 15 kW to 764 V at 18 kW and to 737 V at 21 kW. The power matching is achieved for all the load conditions. The VF control is found to be effectively working as the load line voltage of 440 V rms and the frequency of 50 Hz are maintained.

3.7 ULTRA CAPACITOR SYSTEM

Ultra capacitors also called super capacitors. Capacitance values up to 400 Farads in a single standard case size are commercially available. Super capacitors have the highest capacity density and makes suitable substitute for batteries.

The features of the ultra capacitor are:

- Range from a Farad to thousands of Farads
- High Power density
- Low cost per cycle
- Long life time
- Very high rates of charge and discharge
- Environmentally friendly
- Good reversibility
- Extremely low internal resistance (ESR) and
- Light weight

The most significant advantage of super capacitors over batteries is the ability to charge and discharge continuously without degrading like batteries. (M Jayalakshmi et al. 2008).

3.71 UC Modeling

The figure 3.27 shows equivalent circuit of an ultra capacitor unit, consisting of capacitance C , an equivalent series resistance (ESR) representing the charging and discharging resistance and an equivalent parallel resistance (EPR) representing the self discharging losses. In the model considered, the EPR is neglected as it affects the ultra capacitor in long duration storage (Santhoshakumar A et al. 2011).

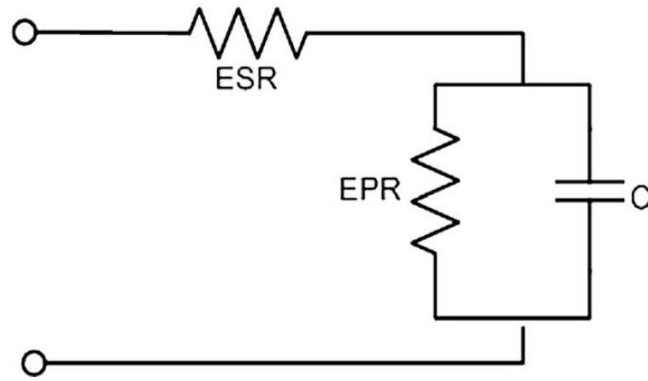


Figure 3.27: Ultra capacitor equivalent circuit.

For an ultra-capacitor bank, the energy E_{uc} is:

$$E_{uc} = \frac{1}{2} C_t (V_{max}^2 - V_{min}^2) \quad (4.1)$$

The total capacitance, C_T and series resistance, ESR_T are given by 4.2 and 4.3 equations:

$$C_T = \frac{N_p}{N_s} C_{uc} \quad (4.2)$$

$$ESR_T = \frac{N_s}{N_p} ESR_{uc} \quad (4.3)$$

$$N_s = \frac{V_{max}}{V_{uc}} \quad (4.4)$$

Where

- N_s is the number of individual capacitor connected in series,
- N_p is the number of capacitor branches connected in parallel,
- V_{uc} is individual capacitor voltage and
- C_{uc} is the individual capacitance value of the capacitor.

3.72 Bidirectional DC-DC Converter

There will be noticeable power transients at DC bus, resulted due to both the variation in loads and others due to change in environmental conditions. These variations in power will be reflected as change in DC bus voltage. To mitigate these

variations, UC system is connected to DC bus through a bidirectional converter. Bidirectional converter will facilitate power absorption as well as power feed. The schematic of the bidirectional converter is as shown in figure 3.28 (Prashant Kumar Soori et al. 2011).

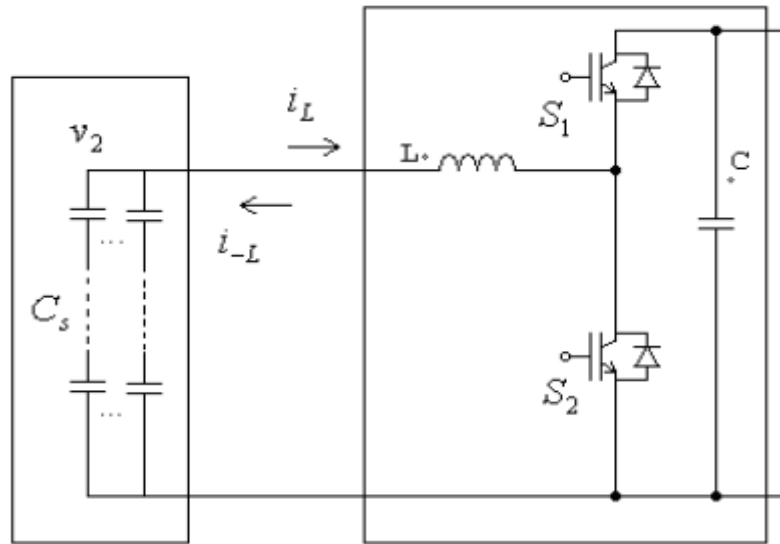


Figure 3.28: Bidirectional DC-DC converter

Where C is the dc link capacitance and C_s is the super capacitor bank. The control scheme for the converter is as shown in the figure 3.29.

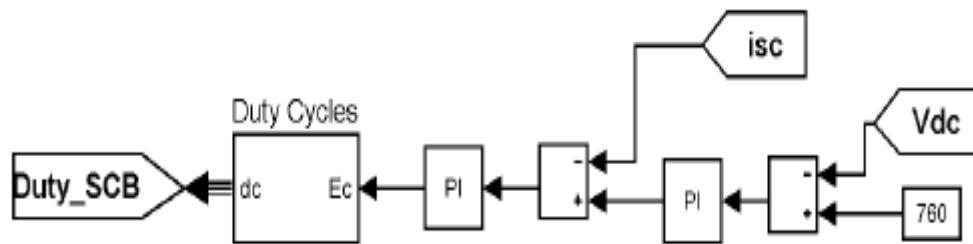


Figure 3.29: Bidirectional dc-dc converter control system.

The control strategy involves an outer loop of voltage control with reference signal I_{ref} which is obtained by comparing the actual DC bus voltage with reference DC voltage. Then, in the inner loop I_{ref} is compared to ultra-capacitor current I_{UC} . Thus, a double loop control is realized for better stability. Then the PI generated control signals are given to PWM generators which develop two mutually exclusive set of duty ratios for the two switches viz. Switch 1 and Switch 2 (Jae Hoon Cho et al. 2010).

CHAPTER 4

HYBRID SYSTEM

Normally, PV supplies the power required by the load. The output of the PV changes due to various reasons like temperature, irradiation, etc. If the load is more than PV power capability, micro turbine supplies the remaining power. Micro turbine is a typical and practical solution because of its environment friendliness, small in size and high energy efficiency. Due to the varying load conditions, to reduce the fast fluctuations of power, it is necessary to use an energy storage system like battery, super capacitor, flywheel, etc. An ultra capacitor has been chosen to form the energy storage system, taking advantage of high power density of super capacitor and fast energy storing capability (M. Cacciato et al. 2004).

The Photo voltaic (PV) system consists of the PV array, which gives the DC power under varying temperature and irradiation conditions. The PV array should be connected to the DC grid but the PV output voltage is less than DC grid voltage. So a DC- DC Boost converter, which boosts the PV output voltage to the DC grid voltage, is to be used for connecting the PV model to the grid.

The Micro turbine generator system consists of Micro turbine, PMSG, 3 phase diode bridge rectifier and Buck converter. Micro turbine generator gives AC output but at very high frequency, so a 3 phase full bridge diode rectifier is used for converting AC to DC. DC – DC Buck converter is used for giving a constant DC grid voltage as output, so that the rectified output can be connected to the DC grid.

The ultra capacitor bank is connected to the DC grid using a bidirectional dc-dc converter. The UC bank is used for maintaining constant voltage under varying load conditions.

A 3ϕ inverter is used for converting the DC power to AC. A LC low pass filter is used to reduce the harmonics in the AC output of inverter. The load is connected to the AC bus. The AC bus is not connected to grid as this is a standalone system. The hybrid PV/MTG/UC standalone system is as shown in the figure 4.1.

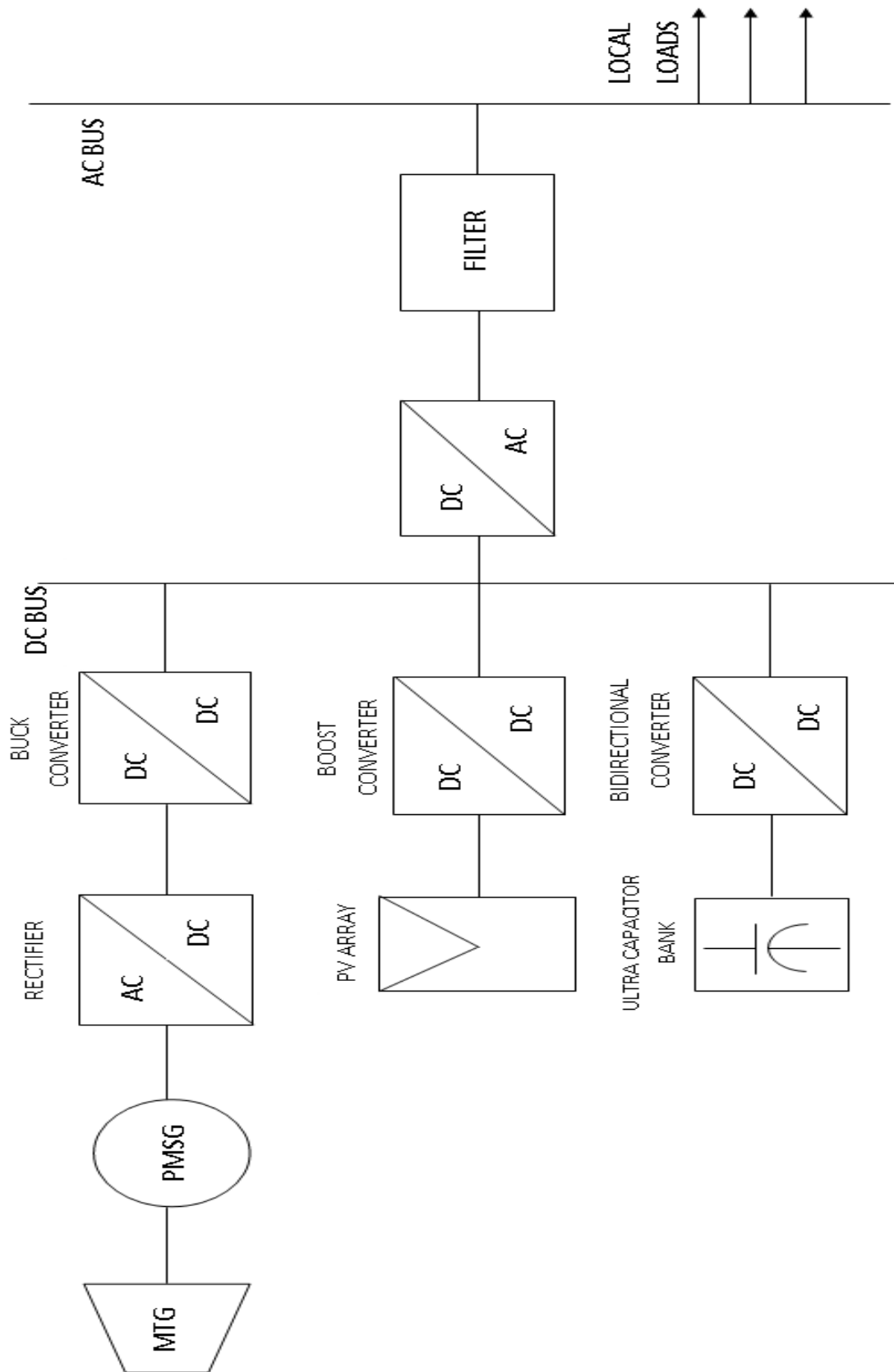


Fig 4.1: hybrid standalone system involving PV/MTG/UC

4.1 PV/MTG/UCHybrid System

A 6 kW PV system is connected in parallel with 21 kW MTG system. The DC output of the boost converter in PV system is connected to the DC link of the MTG system. Since the connection can be done only at common DC voltage, the output of the rectifier in MTG is connected to a buck converter with PI control. The PI control regulates the MTG system DC voltage to a lower level of 700 V. The ultra capacitor bank is connected to the DC link using a bi directional DC –DC converter. A double PI control loop for voltage and current is used for control of bidirectional DC-DC converter. The line voltage is 440 V rms and frequency 50 Hz. The hybrid system of standalone PV / MTG/ UC is implemented in simulink as shown in figure 4.2.

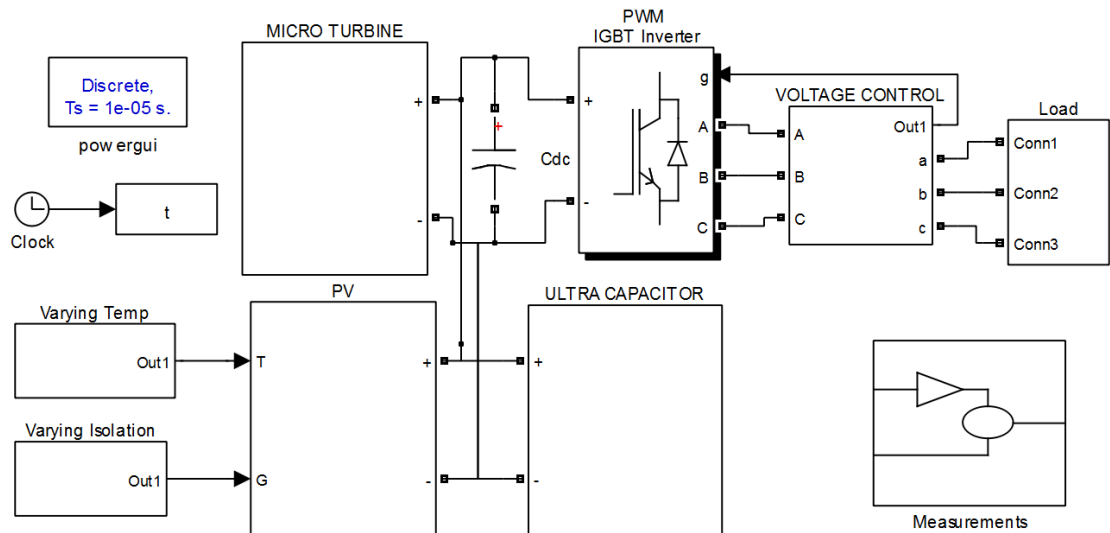


Figure 4.2: PV/MTG/UC hybrid system

The micro turbine subsystem is shown in figure 4.3.

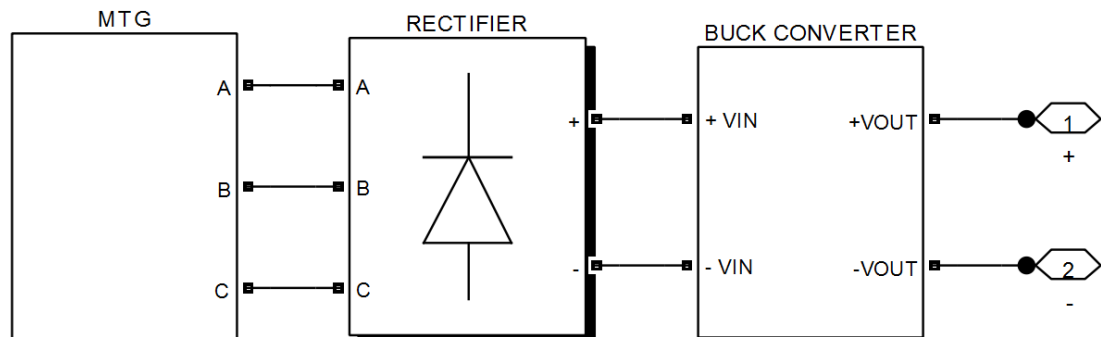


Figure 4.3: The Micro turbine subsystem

The buck converter is implemented as shown in figure 4.4 and its control using PI controller is shown in figure 4.5.

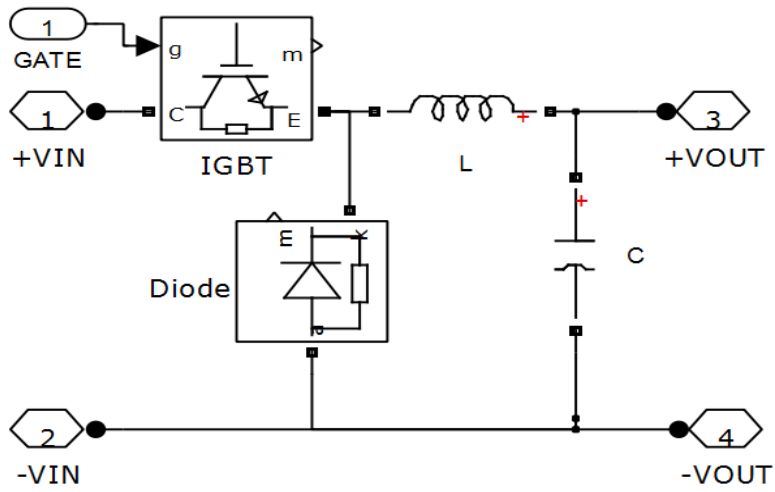


Figure 4.4: Buck converter simulink model

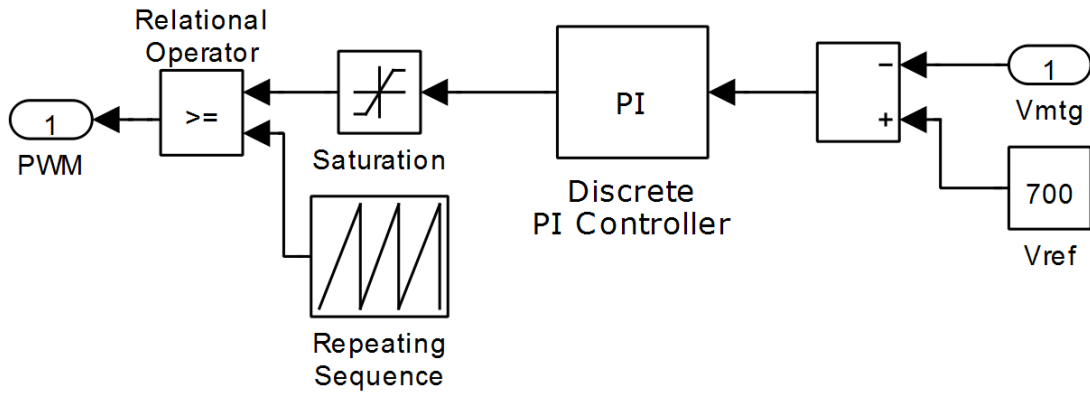


Figure 4.5: Buck converter PI control simulink model

The ultra capacitor subsystem is implemented as shown in figure 4.6.

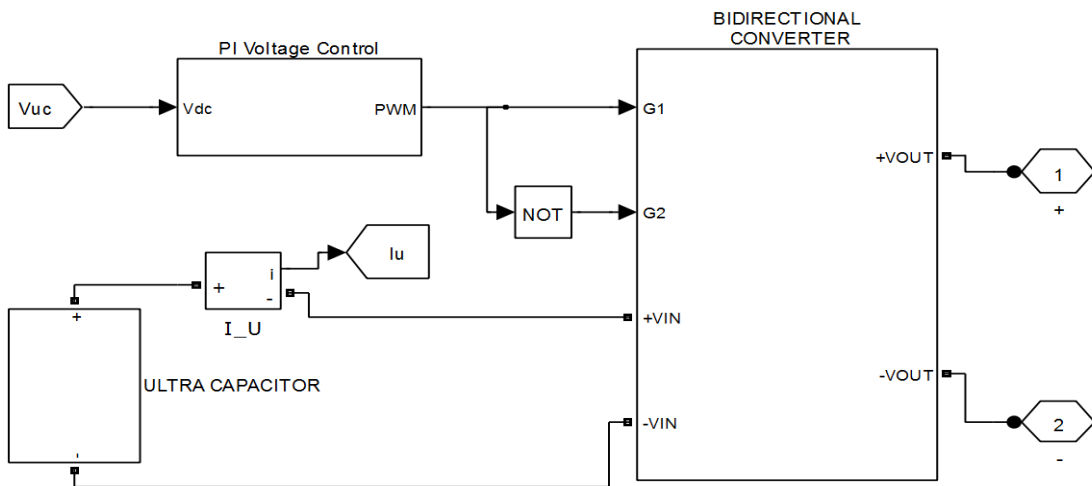


Figure 4.6: Ultra capacitor subsystem

The ultra capacitor bank model is shown in figure 4.7 and the bidirectional converter and its PI control system is implemented in simulink as shown in figures 4.8 and 4.9.

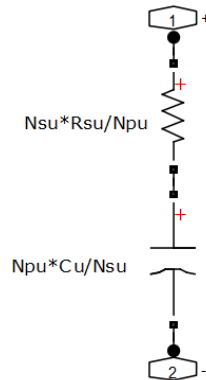


Figure 4.7: Ultra capacitor bank model

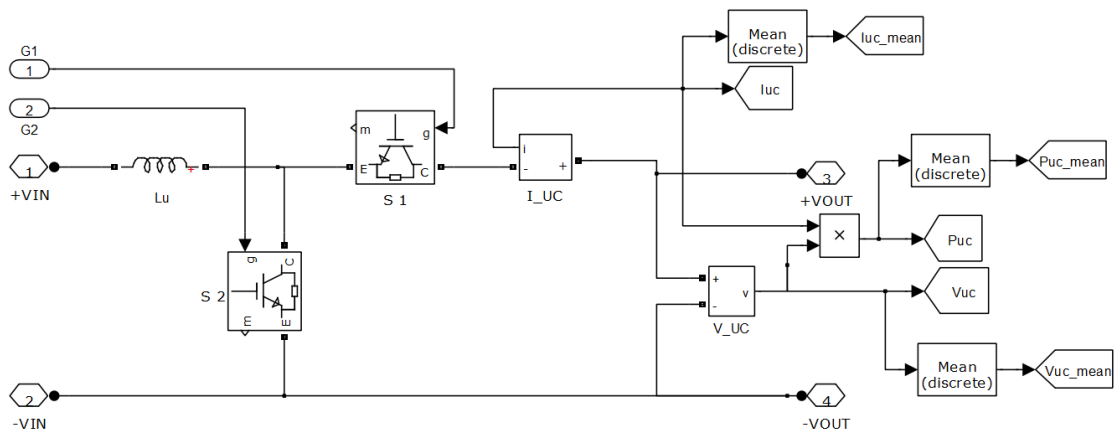


Figure 4.8: Bidirectional DC-DC converter

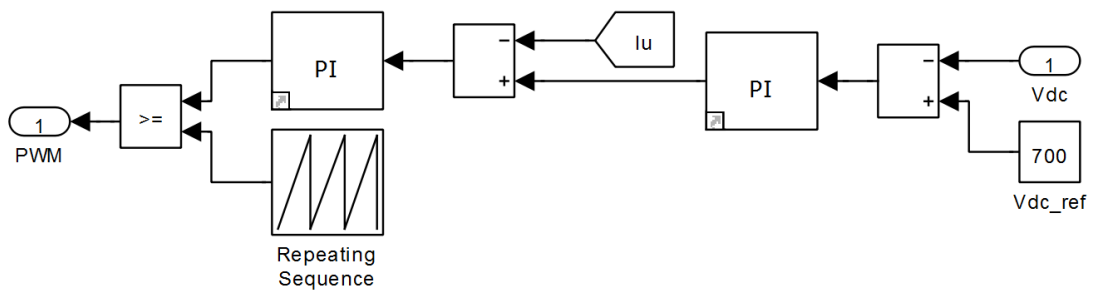


Figure 4.9: Bidirectional DC-DC converter control model

The inverter control is done by VF control as this is a standalone system. The VF control is implemented in SIMULINK as shown in figure 4.10.

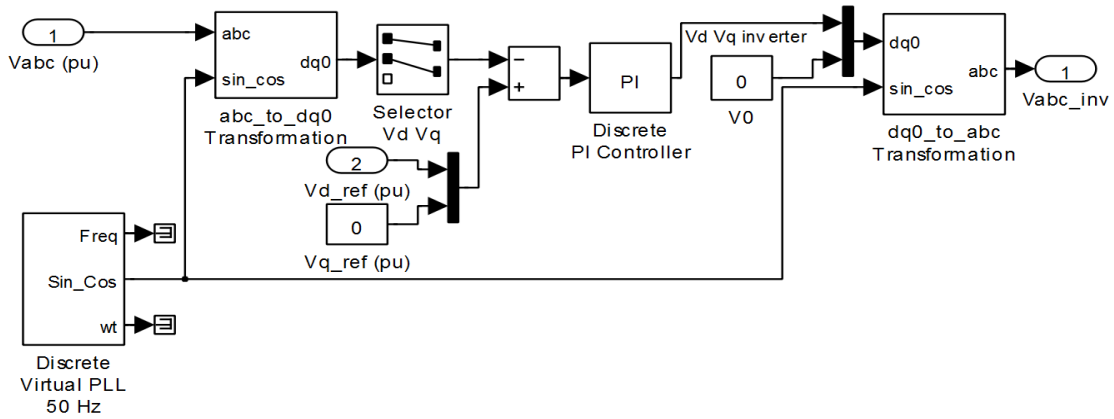


Figure 4.10: VF control

DC link capacitor is used as a load-balancing energy storage device. The DC link capacitor is placed between the DC and the AC (which is the load side) of the voltage inverter. The capacitor maintains a constant voltage across the inverter. The device helps protecting the inverter network from momentary voltage spikes, surges and EMI. The noise is the result of the pulsed inverter current and stray inductance on the DC bus. Cdc is serving as a dc bus and thus, clamping the voltage at the specified value.

The dc-link voltage, however, fluctuates in transient states, according to releasing or absorbing the energy. Thus, the dc-link capacitor can be designed to mitigate the fluctuation of the dc-link voltage. It is with the assumption that the dc-link capacitor releases the transient-state active power, while the shunt device supplies only the steady-state active power. The required capacitance of the dc-link capacitor can be obtained using the following expression.

$$C_{dc} = \frac{3L(I_1^2 - I_0^2)}{2\epsilon V_{dc0}^2}$$

The temperature is varied from 25°C – 45°C and the irradiance is also varied from 400 – 800 W/m². The MPPT and PV output voltages, current and power are obtained as shown in figures 4.11 and 4.12.

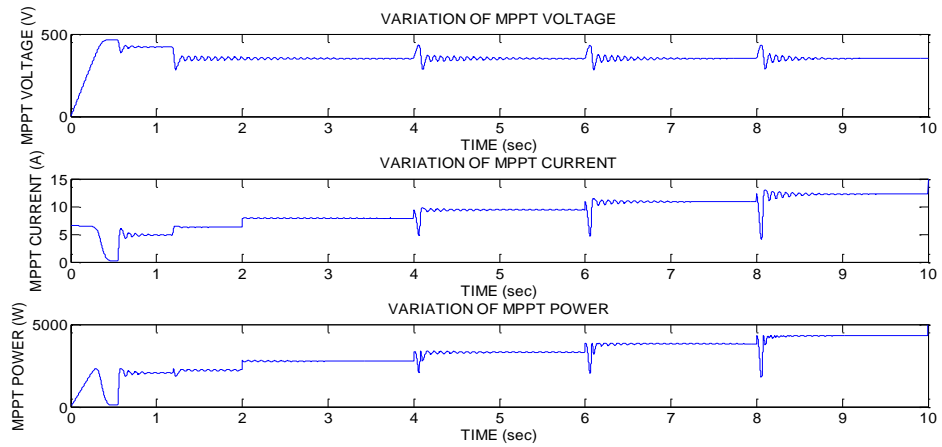


Figure 4.11: MPPT voltage, current and power waveforms.

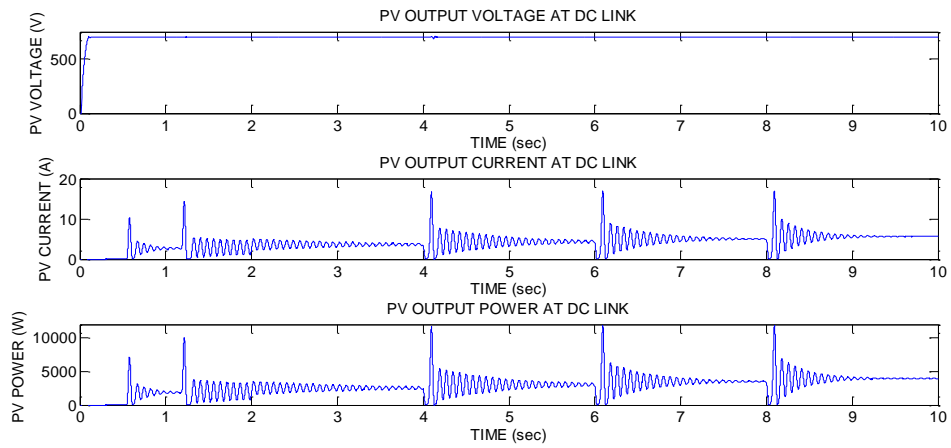


Figure 4.12: PV output voltage, current and power waveforms.

The MPPT is used to track the MPP with 98% efficiency and the PV output power is around 92% . The load is varied from 15 kW at $t=0$ to 20 kW at $t=5$. The PV is primary and MTG is secondary source. The deficit power is given by MTG. The Speed, torque and power of MTG system are as shown in figure 4.13.

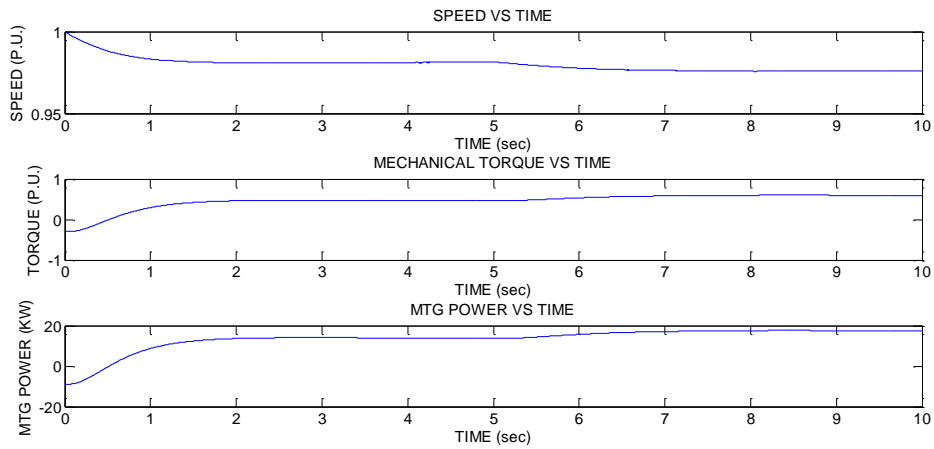


Figure 4.13: Speed, torque and power of MTG

The speed of the MTG drops to 0.981 p.u. for 15 kW and 0.976 for 20 kW.

The fuel demand is 0.588 for 15 kW and 0.679 for 20 kW.

The MTG output voltages, current and power are as shown in figure 4.14.

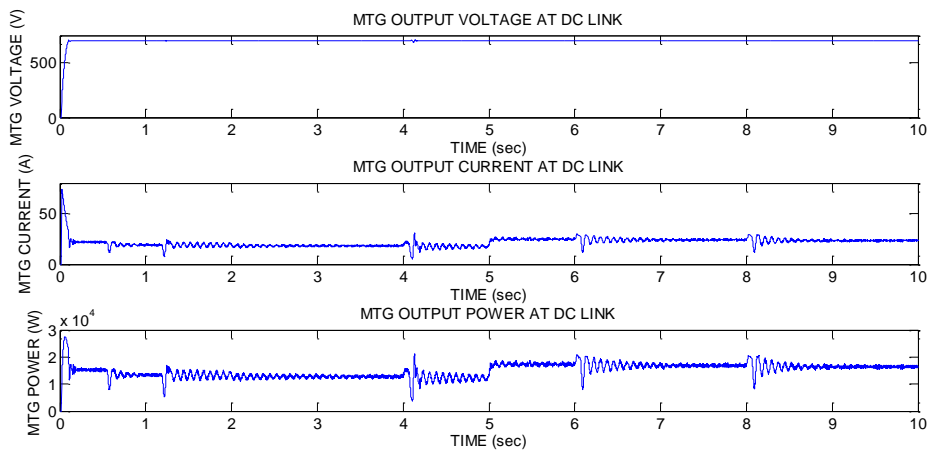


Figure 4.14: MTG output voltages, current and power.

The Ultra capacitor voltages, current and power are as shown in figure 4.15. The ultra capacitor makes the DC link voltage to be constant at 700 V.

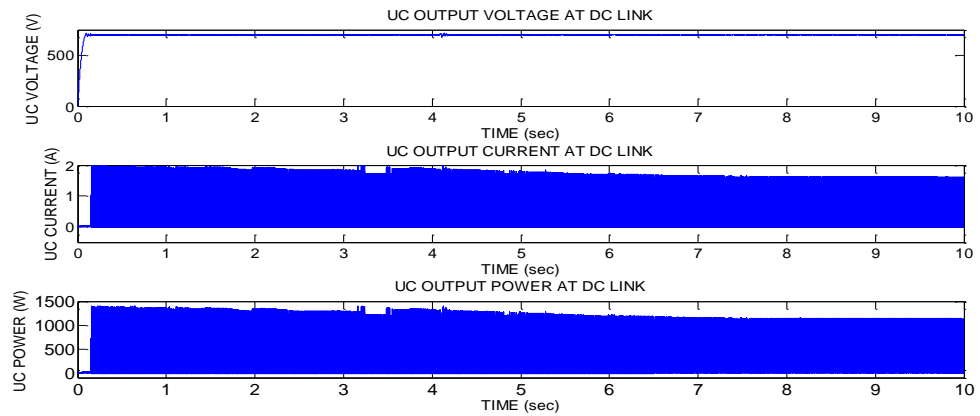


Figure 4.15: Ultra capacitor voltages, current and power.

The inverter V_{ab} line voltage and a part of the V_{ab} are shown in figure 4.16.

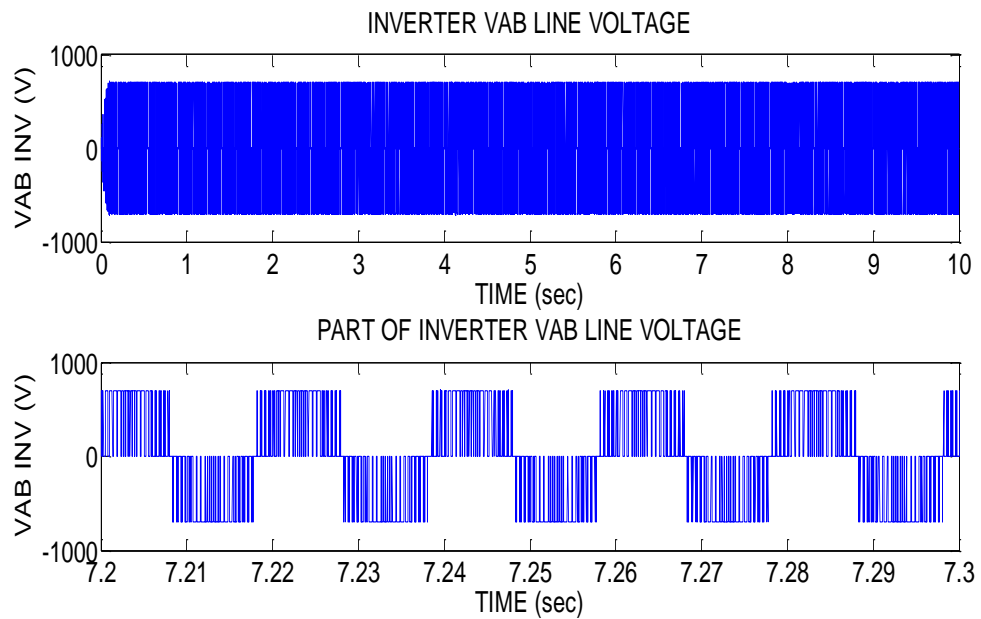


Figure 4.16: Inverter Vab line voltage.

The load phase voltage V_{abc} and phase current I_{abc} and a part of V_{abc} and I_{abc} at 7.2 second to 7.3 seconds are shown in figures 4.17 and 4.18 respectively.

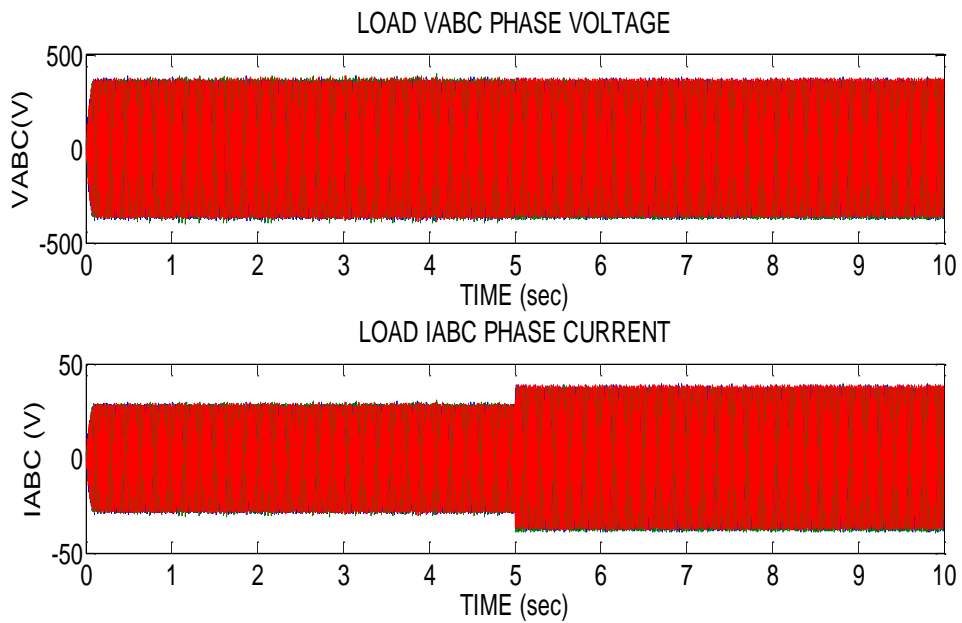


Figure 4.17: Load Vabc and Iabc waveforms.

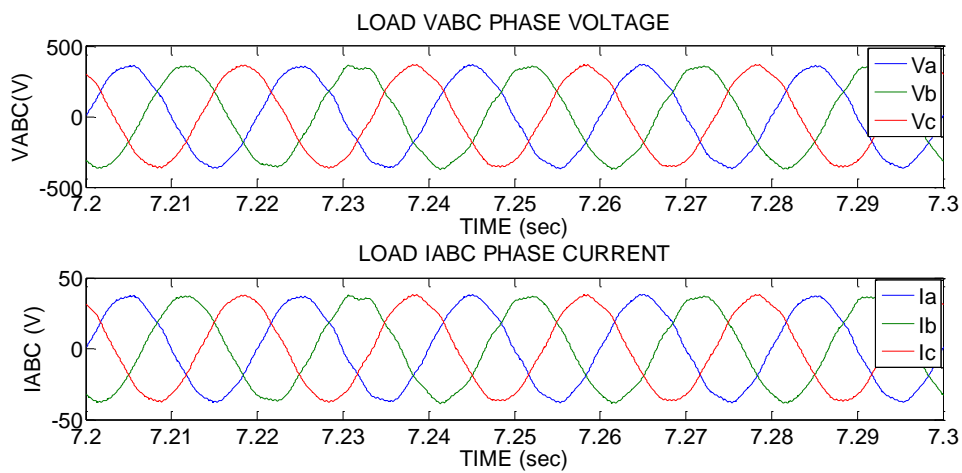


Figure 4.18: Part of Vabc and Iabc

Fourier spectrum for line voltage is as shown in figure 4.19 with THD 3.99%.

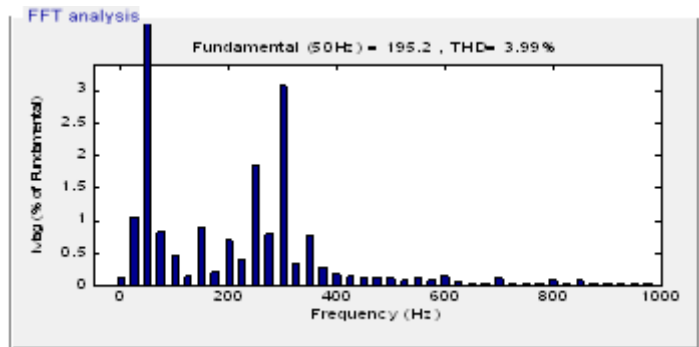


Figure 4.19: Fourier spectrum of line voltage

The load power PQ is as shown in figure 4.20. The load matching is done as per the requirement i.e. 15 kW for first 5 seconds and 20 kW for the next 5 seconds.

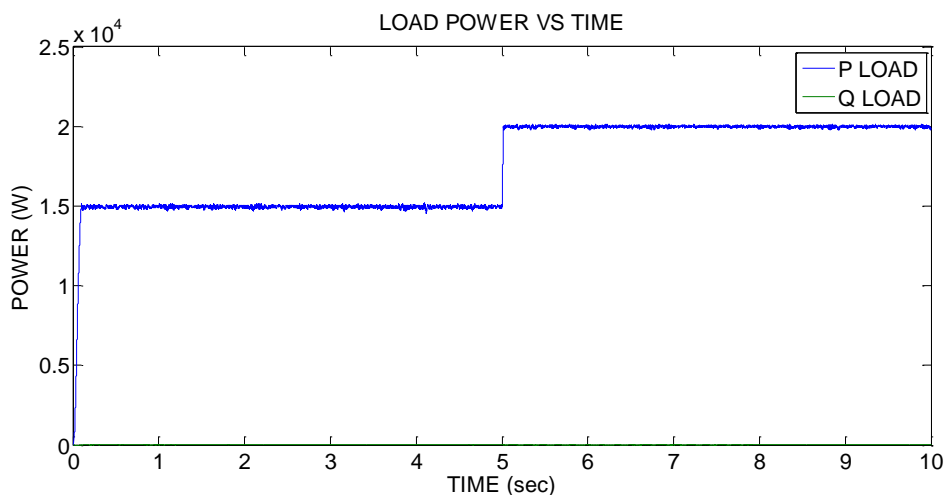


Figure 4.20: Load power PQ

The voltage at the DC bus is constant at 700 V. The MPPT is used to track the MPP with 98% efficiency and the PV output power is around 92 % . The MTG is generating the deficit power to meet the load requirement. The speed of the MTG drops to 0.981 p.u. for 15 kW and 0.976 for 20 kW. The fuel demand is 0.588 for 15 kW and 0.679 for 20 kW. The ultra capacitor makes the DC link voltage to be constant at 700 V. Thus, the standalone PV/MTG/UC hybrid system is implemented effectively.

4.2 PV/MTG Hybrid System

The only difference between the PV/MTG/UC hybrid system and PV/MTG hybrid system is that, there is no ultra capacitor bank connected to the PV/MTG hybrid system. All other models and their parameters are the same. The Simulink model of the PV/MTG hybrid system is shown in the figure 4.21.

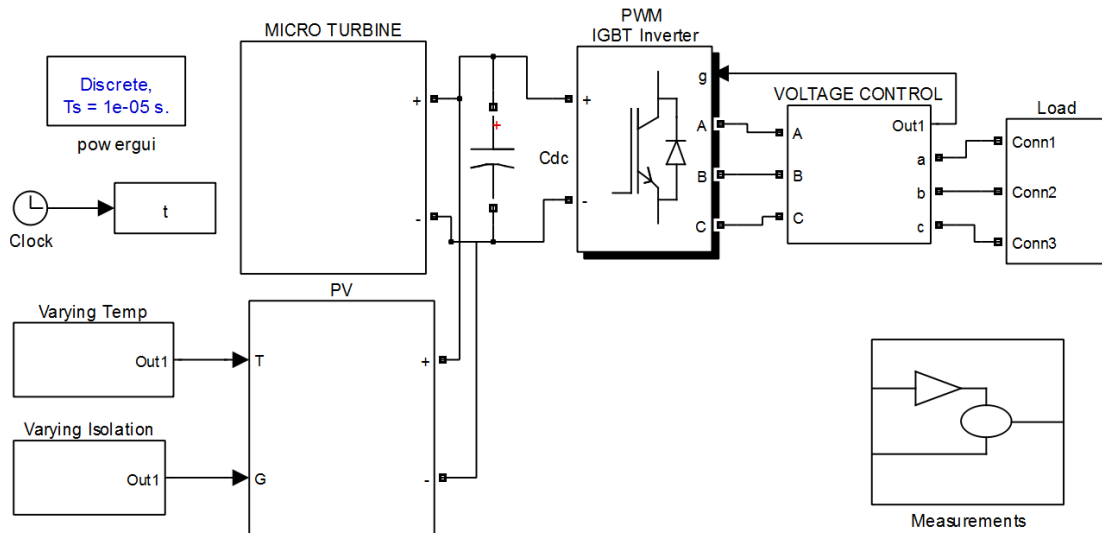


Figure 4.21: PV/MTG hybrid system Simulink model

The voltage at the DC link varies a little bit but all the remaining parameters, like speed, torque, load and inverter voltages are same. The comparison of the voltage at DC link in PV/MTG hybrid system and PV/MTG/UC hybrid system is as shown in figure 4.22.

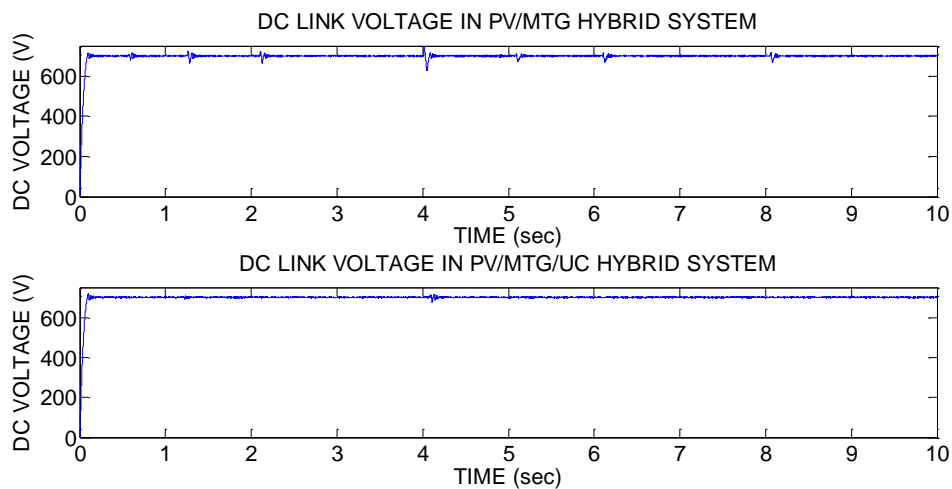


Figure 4.22: Comparison of DC link voltages

CHAPTER 5

CONCLUSION AND FUTURE SCOPE

5.1 Recap of work done

The available power from the solar PV system is highly flexible as it depends on the environmental conditions such as radiation and ambient temperature. The output voltage fluctuations of the solar cell varying with both temperature and irradiation are reduced by using tracking arrangement. In spite of this, the flexibility prevails to certain extent. Further, Sustainable power can be obtained by integrating solar PV generation with a micro turbine generation system. It is clear from the simulation results that the integrated system delivers power to the load with almost constant terminal voltage thus, validating the proposal.

The use of ultra capacitor bank almost reduced the voltage fluctuations. Therefore, the system can tolerate the sudden changes in the load and environmental conditions, and suppress the effects of these fluctuations on the load side voltage.

The standalone PV/ MTG/ UC hybrid system is integrated using power electronic devices, feeding an AC load, and simulated in MATLAB/Simulink. Also, simulation results exhibit that the power electronics interfacing help maintaining the output voltage and frequency of the 3-phase inverter at the specified values during the entire period of operation and the integrated system generates and supplies matching power in sustainable way.

Thus, the work justifies the integration of renewable based energy sources to get sustainable power through the results obtained from the model simulation.

5.2 Scope for future work

Based on the work done in this thesis, the following suggestions are given for future work:

- Grid integration of the hybrid power system can be done to improve the reliability of power supply.
- More renewable energy such as wind, fuel cell, small hydro and biogas etc. can be integrated into the hybrid system.
- Along with ultra capacitor, the battery system can also be connected as long term storage element.
- The distorted current will affect the efficiency, symmetry of the wave and increases THD. However, the capability of multiple pole design, low weight and volume associated with the PMSG can be key drivers in order to deal with reduction in distorted currents. Hence, there is a scope to work on computation of THD and further minimization of THD.

APPENDIX

PV Boost Converter Parameters

- $L = 7 \text{ mH}$,
- $C = 50 \text{ } \mu\text{F}$,
- $C_1 = 5000 \text{ } \mu\text{F}$,
- Switching frequency = 10 KHz.

Incremental Conductance Parameters

- $K_p = 0$,
- $K_i = 7$,
- Error margin = 0.02.

Micro Turbine System Parameters

- Combustor delay = 0.01,

PMSG Parameters

- $R = 0.25 \text{ Ohms}$,
- Pole pairs = 1,
- $L_d = L_q = 0.6875 \text{ mH}$,
- $\lambda = 0.0534 \text{ Wb}$,
- $J = 0.006 \text{ Kgm}^2$.

Inverter Parameters

- Switch: IGBT/DIODE
- $K_p = 0.4$
- $K_i = 500$
- Switching frequency = 2 KHz.

MTG Buck Converter Parameters

- $K_p = 0.001$,
- $K_i = 1$,
- $L = 4 \text{ mH}$,
- $C = 10 \text{ } \mu\text{F}$,
- Switching frequency = 10 KHz.

Filter Parameters

- $L = 2 \text{ mH}$,

- $Q_c = 10 \text{ Kvar}$.

Ultra Capacitor Bank Parameters

- Series resistance of single UC (R_{su}) = $0.29 \text{ m}\Omega$,
- Capacitance of single UC (C_u) = 15.6771 F ,
- Voltage of single UC (V_u) = 2.7 V ,
- Number of UC's in series (N_{su}) = 140 ,
- Number of UC's in parallel (N_{pu}) = 1 ,
- UC bank capacitance (C_t) = 0.1120 F ,
- UC bank capacitance (R_t) = $40.6 \text{ m}\Omega$.

Bidirectional DC-DC Converter Parameters

- $L_u = 7 \text{ mH}$,
- Switching frequency = 10 KHz ,
- $K_p = 0.01$,
- $K_i = 1$.

REFERENCES

Adelmo Ortiz-Conde, Francisco J. Garcia Sanchez, Juan Muci (2006), “New method to extract the model parameters of solar cells from the explicit analytic solutions of their illuminated I–V characteristics”, *Elsevier Solar Energy Materials & Solar Cells*, 90, 352–361.

Ahmed M. Kassem, Almoataz Y. Abdelaziz,(2014), “Reactive power control for voltage stability of standalone hybrid wind–diesel power system based on functional model predictive control”, *IET Renewable Power Generation*, 10.1049/iet-rpg.2013.0199.

Azadeh Safari, SaadMekhilef (2011), “Simulation and Hardware Implementation of Incremental Conductance MPPT With Direct Control Method Using Cuk Converter”, *IEEE Transactions on Industrial Electronics*, (58), 4, 115-1161.

Bhim Singh, M. Rezkallah, Shailendra Sharma and Ambrish Chandra,(2016), “Implementation and Control of Small-Scale Hybrid Standalone Power generation System Employing Wind and Solar Energy”, *Proc IEEE Industry applications conference*, Portland,USA,978-985.

D. N. Gaonkar and R. N. Patel (2006), “Modelling and simulation of micro turbine based distributed generation system”, *Proc IEEE Power India conference*, New-Delhi, India, 256-260.

D. N. Gaonkar and Sanjeev Nayak (2011), “Modelling and Performance Analysis of Microturbine Based Distributed Generation System, A review”, *IEEE Energy tech*, Cleveland, US, 1-6.

Godswill Ofualagba (2012), “The Modeling and Simulation of a Micro turbine Generation System”, *International Journal of Scientific & Engineering Research*,(2), 2, 1-7.

Hassan Nikkhajoei, and M Reza Iravani (2005), "A Matrix converter based micro turbine distributed generation system", *IEEE Transaction on Power Delivery*, (20), 3, 2182-2192.

Jae Hoon Cho and Won-Pyo Hong (2010), “Power control and modelling of a solar ultra capacitor hybrid energy system for stand-alone applications”, International Conference on Control, Automation and Systems, Gyeonggi-do, Korea, 811- 814.

KashifIshaque, Zainal Salam, HamedTaheri, Amir Shamsudin (2011), “A critical evaluation of EA computational methods for Photovoltaic cell parameter extraction based on two diode model” *Elsevier Solar Energy*,(85), 1768–1779 .

Kensuke Nishiokaa, NobuhiroSakitanib, YukiharuUraokab, Takashi Fuyukib (2007), “Analysis of multicrystalline silicon solar cells by modified 3-diode equivalent circuit model taking leakage current through periphery into consideration”, *Elsevier Solar Energy Materials & Solar Cells*, (9), 1222–1227.

Marcelo Gradella Villalva, Jonas Rafael Gazoli and Ernesto RuppertFilho (2009), “Comprehensive Approach to Modelling and Simulation of Photovoltaic Arrays”, *IEEE Transactions on Power Electronics*, (24), 5, 1198-1208.

M. Haouari-Merbaha, M. Belhamelb, I. Tobiasa, J.M. Ruiza (2005), “Extraction and analysis of solar cell parameters from the illuminated current–voltage curve”, *Elsevier Solar Energy Materials & Solar Cells*, 87, 225–233.

M Jayalakshmi, K Balasubramanian (2008), “Simple Capacitors to Super capacitors - An Overview”, *Int. Journ.onElectrochem. Sci.*,(3), 1196 – 1217.

Muhammad H. Rashid (2001), “Power Electronics Handbook”, Academic press, San Diego, California, USA.

M. Zagrouba, A. Sellami, M. Bouaicha, M. Ksouri (2010), “Identification of PV solar cells and modules parameters using the genetic algorithms: Application to maximum power extraction”, *Elsevier Solar Energy*, 84, 860–866.

NevzatOnat (2010), “Recent Developments in Maximum Power Point Tracking Technologies for Photovoltaic Systems”, *International Journal of Photo energy*,(1), 245316, 1-11.

Prashant Kumar Soori, Subhas Chandra Shetty, SibiChacko (2011), “Application Of Super Capacitor Energy Storage In Microgrid System”, *IEEE GCC Conference And Exhibition*, Dubai, UAE, 581-584.

Santhoshakumar A, D.N. Gaonkar and Sanjeev K Nayak (2011), “ Performance Study of Grid Connected Fuel Cell Based Distributed Generation System with Ultra capacitor”, *IEEE PES Conference on Innovative Smart Grid Technologies*, Jeddah, Saudi Arabia, 1- 4.

Soon Kiat Yee, Jovica V. Milanovic and F. Michael Hughes (2008), “Overview and Comparative Analysis of Gas Turbine Models for System Stability Studies”, *IEEE Transactions on Power Systems*, (23), 1, 108-118.

S. R. Guda, C. Wang and M. H. Nehrir (2005), “Modelling of micro turbine power generation systems”, *Electrical Power System and Components*, (34), 9, 1027-1041.

TrishanEsram, Patrick L. Chapman (2007), “Comparison of Photovoltaic Array Maximum Power Point Tracking Techniques”, *IEEE Transactions on Energy Conversion*, (22), 2, 439-449.

Ulrich Stutenbaeumer, Belayneh Mesfin (1999),“Equivalent model of mono crystalline, poly crystalline and amorphous silicon solar cells”, *Elsevier Renewable Energy*, 18, 501-512.

Xiaofeng Sun, Yanfeng Shen, (2015),“ A PWM and PFM Hybrid Modulated Three-Port Converter for a Standalone PV/Battery Power”, *IEEE Journal of Emerging and Selected topics in Power Electronics*, (3),4, 984-1000.

Yousef Mahmoud, W. Xiao and H. H. Zeineldin (2012), “A Simple Approach to Modelling and Simulation of Photovoltaic Modules”, *IEEE Transactions on Sustainable Energy*, (3),1, 185-186.

LIST OF PUBLICATIONS

REFEREED JOURNALS

1. **Basavaraj Shalavadi.**, Ravindranadh Vankina ,and Udaykumar, R.Y. (2016)
“ *Modelling and Analysis of a Standalone PV/Micro Turbine/Ultra Capacitor Hybrid System* ”, *International Journal of Renewable Energy Research (IJRER)*,(6), 3, 847-855.

CONFERENCE PROCEEDINGS

1. **Basavaraj Shalavadi.**, Ravindranadh V, and Udaykumar, R.Y. (2017)
“*Modelling and Analysis of a Standalone PV/Micro Turbine Hybrid System*”,
Proceedings of the IEEE International Conference on Innovative Mechanisms for Industry Applications. (ICIMIA 2017), 774-779. Bangalore, India.-
Conferred BEST PAPER AWARD

CURRICULUM VITAE

Mr. Basavaraj .S. Shalavadi is a research scholar in the Department of Electrical & Electronics Engineering, National Institute of Technology Karnataka (NITK), Surathkal, Mangalore, INDIA. He obtained Bachelor's degree in Electrical and Electronics Engineering from Malnad College of Engineering (MCE) Hassan, Mysore University, in the year 2000 with First Class. He holds Master's degree in Electrical Energy Systems from VTU University, Belgaum in the year 2004 with First Class Distinction. After his Master's degree, he is working as an Assistant Professor in Department of Electrical and Electronics Engineering, SDM College of Engineering and Technology, Dharwad. He has 14 years of teaching experience. His fields of interest are Energy management, Energy audit, Energy systems.

Address:

Mr. Basavaraj .S. Shalavadi
Assistant Professor,
Department of Electrical & Electronics Engineering,
SDM College of Engineering and Technology,
Dharwad, Karnataka-580002, INDIA.
Phone:+91-9448433561
Email: shalavadibs@gmail.com